NASA TECHNICAL NOTE

NASA TN D-3856

WIND-TUNNEL INVESTIGATION OF THE STATIC AERODYNAMIC CHARACTERISTICS OF AN 18-FOOT (5.49-METER) ALL-FLEXIBLE PARAWING

by Charles E. Libbey, George M. Ware, and Rodger L. Naeseth

Langley Research Center
Langley Station, Hampton, Va.

NATIONAL AERONAUTICS AND SPACE ADMINISTRATION • WASHINGTON, D. C. • JUNE 1967

WIND-TUNNEL INVESTIGATION OF THE STATIC AERODYNAMIC CHARACTERISTICS OF AN 18-FOOT (5.49-METER) ALL-FLEXIBLE PARAWING

By Charles E. Libbey, George M. Ware,
and Rodger L. Naeseth

Langley Research Center
Langley Station, Hampton, Va.

NATIONAL AERONAUTICS AND SPACE ADMINISTRATION

For sale by the Clearinghouse for Federal Scientific and Technical Information
Springfield, Virginia 22151 – CFSTI price $3.00

WIND-TUNNEL INVESTIGATION OF THE STATIC AERODYNAMIC CHARACTERISTICS OF AN 18-FOOT (5.49-METER) ALL-FLEXIBLE PARAWING

By Charles E. Libbey, George M. Ware,
and Rodger L. Naeseth
Langley Research Center

SUMMARY

An investigation has been conducted in the Langley full-scale tunnel to determine the performance and the static stability and control characteristics of an 18-foot (5.49-meter) all-flexible parawing. This parawing had no rigid structural members and utilized only the tension forces produced by the aerodynamic loading to maintain the shape of the canopy. The tests showed that the parawing was longitudinally stable at angles of attack from about 30° to 40°. In this angle-of-attack range the parawing could be trimmed longitudinally over a range of lift-drag ratios from about 2.0 to 1.5. At lower values of lift-drag ratio, which correspond to angles of attack above 40°, there was a destabilizing break in the pitching-moment curve and the parawing was unstable over the remainder of the test angle-of-attack range (up to 100°). As the angle of attack was decreased below 30°, the nose portion of the wing collapsed, and at an angle of attack near 28° the entire wing collapsed. The wing, however, could be reinflated by increasing the angle of attack. The parawing was directionally stable and had positive effective dihedral over most of the test angle-of-attack range but was directionally unstable and had negative effective dihedral at angles of attack from about 35° to 45°. Differential deflection of the wing tips for lateral control produced positive rolling moments and negative yawing moments over most of the test angle-of-attack range when the lines were changed in a direction to lower the right wing tip. This result would be expected from a center-of-gravity shift type of control.

INTRODUCTION

There is, at the present time, an increasing interest in gliding parachutes as a means of space-vehicle recovery and cargo delivery; and there are a number of different types of gliding parachutes being developed to meet the demand for such a system. In order to evaluate the performance, stability and control, and deployment characteristics of this type of configuration, the Langley Research Center is presently evaluating several parachute-like devices with gliding capability by means of wind-tunnel and flight tests.

One concept in the gliding parachute category which has received considerable attention is a parawing completely void of any rigid structural members and utilizing only the tension forces produced by the aerodynamic loading to maintain the shape of the canopy. This device, which was developed at the NASA Langley Research Center, is called an all-flexible parawing. The particular wing used in the present investigation had a modified 45° delta planform with suspension lines along the keel and leading edges and has demonstrated free-flight capability. The investigation consisted of static wind-tunnel force tests to determine the basic lift and drag characteristics and the longitudinal and lateral stability and control characteristics of such a parawing over an angle-of-attack range from 30° to 100° and at sideslip angles up to 10°. These tests were conducted at several different values of dynamic pressure to evaluate the effects of wing loading in simulated steady trimmed gliding flight (lg) conditions.

SYMBOLS

The data are referred to the stability system of axes. The origin of the axes was located to correspond to a center-of-gravity position at the confluence point of the model suspension lines. The coefficients are based on the laid-out-flat canopy area of 224 square feet (20.8 square meters), keel length of 15.75 feet (4.8 meters), and wing span of 25.45 feet (7.76 meters). Measurements used in this investigation were taken in the U.S. Customary System of Units. Equivalent values are indicated parenthetically herein in the International System of Units (SI). Details of the system together with conversion factors can be obtained in reference 1.

b wing span, feet (meters)

C_D drag coefficient, $\frac{D}{qS}$

C_L lift coefficient, $\frac{L}{qS}$

C_l rolling-moment coefficient, $\frac{\text{Rolling moment}}{qSb}$

$C_{l_\beta} = \frac{\partial C_l}{\partial \beta}$, per degree

C_m pitching-moment coefficient, $\frac{\text{Pitching moment}}{qSl_k}$

C_n yawing-moment coefficient, $\frac{\text{Yawing moment}}{qSb}$

$C_{n_\beta} = \frac{\partial C_n}{\partial \beta}$, per degree

C_Y side-force coefficient, $\frac{\text{Side force}}{qS}$

$C_{Y_\beta} = \frac{\partial C_Y}{\partial \beta}$, per degree

D drag, pounds (newtons)

F_A axial force, pounds (newtons)

F_N normal force, pounds (newtons)

L lift, pounds (newtons)

L/D lift-drag ratio

l_k keel length, feet (meters)

M moment, foot-pounds (meter-newtons)

M_Y pitching moment, foot-pounds (meter-newtons)

q free-stream dynamic pressure, pounds per square foot (newtons per square meter)

S wing area, square feet (square meters)

x distance between model suspension confluence point and moment center of upper strain-gage balance of support system, feet (meters)

α angle of attack (angle between relative wind and wing chord line perpendicular to streamline strut), degrees

β angle of sideslip, degrees

δ change in length of a suspension line being used as a control, inches (meters); positive value indicates increasing line length

Subscripts:

K-11 keel line

L-6 left wing-tip line

R-6 right wing-tip line

T total

u upper balance

l lower balance

TEST MODEL AND APPARATUS

A plan-view drawing of the parawing canopy in a laid-out-flat condition is presented in figure 1. A sketch and a photograph of the model mounted for force testing in the Langley full-scale tunnel are presented in figures 2 and 3, respectively. Some of the more important items of the test setup are labeled on figure 2. The fabric used to form the membrane of the parawing was 1.1-ounce (31g) per-square-yard (0.037 kg/m^2) rip-stop nylon cloth with an acrylic coating to reduce the porosity to nearly zero. The warp of the cloth was normal to the trailing edge. Twenty-three nylon suspension lines were used to transfer the load from the wing membrane and to control the shape the membrane would assume under aerodynamic loading. Each leading edge had six suspension lines and the keel had eleven suspension lines. (See table I for line spacing.) The length of the suspension lines from the confluence point to the canopy for two test configurations investigated is given in table II. The lengths of the suspension lines for the basic configuration were determined from preliminary free-glide tests. Subsequently, the line lengths were further adjusted to the modified line configuration in an effort to improve the performance of the model.

The mounting arrangement for the parawing consisted of a long streamline strut pivoted in the middle to permit change of angle of attack and with strain-gage balances mounted at both ends. (See fig. 2.) The strain gage at the lower end of the streamline strut was fitted with a yoke to which all the suspension lines were attached. The strain gage at the upper end of the streamline strut was fitted with a short spike which protruded through a small hole in the membrane of the parawing canopy at a point on the keel 60 percent of the theoretical keel length back from the theoretical apex. The spike restrained the parawing from pitching or rolling with respect to the streamline strut with very little apparent distortion to the shape of the canopy. In order to restrain the wing from yawing or to hold the wing at a given sideslip angle, the suspension lines from the keel were passed between two parallel aluminum tubes which were rigidly attached to the streamline strut. With the parawing mounted in this fashion, fabric and line stretch were virtually unaffected and the model was free to assume the shape dictated by the aerodynamic loading. Also, because of the location of the strain-gage balances, the forces and moments measured were independent of the aerodynamic tare forces on the support system. The entire wing support system was mounted on the full-scale-tunnel force-measuring scales, which were used to obtain the lateral aerodynamic characteristics because the strain-gage balances were not instrumented to measure lateral forces. The full-scale-tunnel force-measuring scales also provided a second system for measuring the longitudinal aerodynamic characteristics of the parawing for comparison with data from the strain-gage balances.

Tests

The investigation was conducted in the Langley full-scale tunnel, a complete description of which is given in reference 2. The lift and drag and the static longitudinal stability and control characteristics of the parawing were determined from force measurements obtained from the two-strain-gage system. A schematic drawing showing the forces and moments measured and how they were

resolved into the coefficients of lift, drag, and pitching moment is presented in figure 4. One longitudinal check test and all the lateral tests were made by using the tunnel scale-balance system to record the force-test data. Tests were made for a range of angles of attack (as measured from the angle between a relative wind and a wing-chord line perpendicular to the streamline strut) from about 30° to 100° for several values of control-line length and dynamic pressure. Most of the tests were conducted at a dynamic pressure of 1.00 pound per square foot (47.9 newtons per square meter). Included in the investigation, however, were tests at higher and lower values of dynamic pressure to evaluate the effects of wing loading on the aerodynamic characteristics of the configuration at simulated steady gliding flight conditions. Longitudinal control tests were made with the model in its basic rigging by changing the keel and wing-tip suspension lines as follows:

(a) Keel line was shortened by 4 inches (0.10 meter)

(b) Keel line was lengthened by 4 inches (0.10 meter)

(c) Keel line, left wing-tip line, and right wing-tip line were each shortened by 4 inches (0.10 meter)

The range of dynamic pressure used in the investigation varied from about 0.50 to 1.50 pounds per square foot (24.0 to 71.9 newtons per square meter), which corresponded to an airspeed range from about 20 to 40 feet per second (6.1 to 9.15 meters per second) at standard sea-level conditions. The Reynolds number range covered in the tests varied from about 1.91×10^6 to 3.83×10^6, based on the parawing keel length of 15.75 feet (4.8 meters).

The lateral stability and control tests were made only at a dynamic pressure of 1.00 pound per square foot (47.9 newtons per square meter) at angles of attack from 30° to 70° for an angle-of-sideslip range from -10° to 10°. The lateral control tests were made with total differential lengths of 4 and 8 inches (0.10 and 0.20 meter) in the wing-tip lines for both left and right control inputs.

Corrections

The data are presented with no corrections applied on the basis of the following analysis of the correction problem. In order to obtain some indication of the relative magnitude of the corrections, jet boundary, buoyance, and blockage corrections were determined by use of conventional wind-tunnel methods. It should be pointed out that the all-flexible parawing operates at relatively high angles of attack, whereas the available wind-tunnel correction methods are generally intended to apply to low angle-of-attack conditions. There is, therefore, some reason to question the applicability of standard wind-tunnel corrections in this case, especially at angles of attack near 90°. At the lowest angles of attack where the methods are considered most applicable (and where the maximum values of L/D occurred), the corrections were found to be negligible. Since most of the data were measured at high angles of attack where conventional wind-tunnel correction methods are questionable and since the corrections for the low angle-of-attack conditions were very small, the data are presented with no corrections applied.

RESULTS AND DISCUSSION

Corroboration of Techniques

Hysteresis effects.- In the proposed operation as a recovery device, the all-flexible parawing is intended to be deployed much like a parachute which would give an initial opening angle of attack of about 90°. After the deployment, the wing would rotate to a lower angle of attack and the configuration would go into gliding flight. Most of the force tests were made, therefore, by beginning at a high angle of attack and recording data as the angle was successively reduced. In order to determine whether there was any difference between this test procedure and the more conventional test method of increasing angle of attack, one test was made in which data were taken while the angle of attack was increased, and the results of this test are presented in figure 5. These data show that for the test angle-of-attack range (up to 40°), there were higher values of lift recorded when the model was tested by decreasing angle of attack. The reason for the greater lift was apparent from visual observations. As the angle of attack was decreased below 40°, the nose portion of the parawing began to deform until at about 28° the wing collapsed entirely. In most such cases, when the angle of attack was increased, the wing would reinflate. When the wing was tested by increasing angle of attack, the model was initially positioned at $\alpha = 30^{\circ}$. At this angle the model was somewhat deformed and, as the angle of attack was increased, there was delay in the angle of attack at which the nose section became fully inflated again. This lag in the assumption of the normal nose shape evidently resulted in the lower values of lift.

Comparison of force-measuring systems.- The data obtained from the full-scale-tunnel scale system are compared with the data obtained during the same test with the two-balance strain-gage system in figure 6. These data show that the lift, drag, and lift-drag ratio compare very well for the two systems. The pitching-moment curves do not agree quite so well in actual magnitude, although the slopes and trends are in good agreement. One possible reason for the pitching-moment differences may be attributed to errors in the moment-transfer distances from the full-scale-tunnel scales to the model center of gravity due to the flexing of the support system. Another possible reason for the discrepancy in the magnitude of the pitching moments is believed to be that, because of the tunnel scale system, it was difficult to determine accurately the aerodynamic tare of the support system; and when any relatively small inaccuracies in accounting for lift and drag tares are transferred, the long distances involved in moment transfers for the tunnel scale-balance system, they can yield significant moment errors. The strut tares were measured with the wing off and were used in the reduction of the data. The actual aerodynamic tare of the support system in the presence of the wing may be considerably different from that measured, because the wing can induce a change in velocity over the strut. There are no strut tare corrections with the two-balance system, since in this system only the aerodynamic forces acting on the wing are measured. In both systems there are interference effects of the strut on the wing which have not been taken into account. It should be pointed out that the lateral data, which were measured with the tunnel scale system, are subject to errors in tare corrections similar to those pointed out in the longitudinal case for this measuring system.

Longitudinal Stability and Control

Longitudinal characteristics of the model.- The longitudinal characteristics of the configuration with the basic rigging are presented in figure 7. At angles of attack below about 30° the nose of the configuration with the basic rigging would start to deform, regardless of the test airspeed; as a result, no data were taken below this angle. Actually, as previously pointed out, the wing collapsed at an angle of attack of 28°. As may be seen, the lift was at a maximum and was relatively constant from $\alpha = 30^\circ$ to $\alpha = 40^\circ$ and then decreased at the higher angles of attack. The maximum lift-drag ratio obtained was about 1.9. Indications are, however, that if the nose of the wing had remained inflated at lower angles of attack, somewhat higher values of L/D might have been obtained. The pitching-moment data of figure 7 show that, at angles of attack from 30° to 40°, the slope of the pitching-moment curve was stable, and that the configuration was trimmed at an angle of attack of about 30°, which was approximately the angle for maximum lift-drag ratio. At an angle of attack of about 40° and lift-drag ratio of approximately $1\frac{1}{2}$ the pitching moment showed an unstable break and the configuration was statically unstable at all higher angles of attack.

Because the material from which the parawing was fabricated stretches with load, and because the aerodynamic loads are not evenly distributed, the tests were conducted at the three different values of dynamic pressure shown in figure 7. These tests simulate the wing in a steady trimmed gliding flight condition (1 g) at different wing loadings. The data obtained at the different values of dynamic pressure are generally similar, but at the lowest value of dynamic pressure lower values of lift and drag and a different trim point were measured than for the other two values. This result is probably associated with the fact that, at the lowest value of dynamic pressure, the wing did not appear to fill out as well as it did at the two higher values (particularly along the leading edge and near the nose) because the weight of the wing was sufficiently large in proportion to the lift being produced to cause the wing to sag. This deformation might be expected to have detrimental effects on the aerodynamic characteristics of the wing. The lift-drag ratio of the wing, however, was about the same for all three dynamic pressures in spite of the distortion of the wing at the lowest speed. Tests at a dynamic pressure of 1.5 could only be made at angles of attack up to 40°. At angles of attack of 45° and beyond, the wing began to oscillate so badly that no reliable data could be taken. This occurrence, however, does not indicate that the wing would oscillate at this value of q in free flight. The oscillation was very likely associated with the restraint provided by the mounting system.

Effect of suspension-line rigging.- In an effort to improve the performance of the all-flexible parawing, slight modifications were made to the suspension-line lengths which had the effect of reducing the camber of the canopy. A comparison of the results obtained with the model with the modified and basic suspension-line configurations is presented in figure 8. As may be seen, the model with modified lines remained inflated to a lower angle of attack so that the wing was operating on the unstalled side of the lift curve. In this configuration, the model had a higher value of maximum lift-drag ratio as a result

of the lower angle of attack achieved. The maximum value of lift-drag ratio in this case was 2.1.

Effect of control deflection.- It would be expected that the parawing would be controlled by changing the length of one or more of the suspension lines. The easiest and most obvious arrangement for pitch control is to change the length of the keel line. Figure 9 presents the results of tests in which the length of the keel line was increased and decreased 4 inches (0.10 meter) from its original length. This type of pitch control did not appreciably affect the variation of lift, drag, and lift-drag ratio with angle of attack. It did, however, affect the trim point, as would be expected. It should be noted that the control does not operate in the same sense as an elevator, since pulling down on the trailing edge causes a nose-up pitching moment and caused the wing to trim at a higher angle of attack. Actually, the control acts in the sense of a center-of-gravity shift type of control. Lengthening the keel line 4 inches (0.10 meter) produced a negative trim shift in the pitching-moment curve. With the basic line length, however, the parawing was already trimmed very nearly at the point of collapse so that lengthening the keel line shifted the curve to such an extent that there was no stable trim point in the range of angles of attack where the wing would stay inflated. Shortening the keel line caused the parawing to trim at a slightly higher angle of attack. The data also indicate that because of the unstable break in the pitching-moment curve, a stable trim range for the model with the test-line rigging is possible only from an angle of attack of 30° to about 40°. With this trim range, it would be possible to modulate the lift-drag ratio from about 2.0 to 1.5.

Figure 10 shows the results of shortening the keel line in combination with the two wing-tip lines by 4 inches (0.10 meter) each, as compared with shortening only the keel line by 4 inches (0.10 meter). The data indicate that the combination control produced the greater shift in the pitching-moment curve. This result is as expected, since the whole aft portion of the wing becomes effective as a control.

Comparison of Small-Scale and Large-Scale Wings

In an effort to provide additional information for use in interpreting the results of static longitudinal tests of all-flexible gliding devices, a brief investigation was conducted with a smaller wing and a theoretical keel length of 5 feet (1.52 meters); this wing was an exact scale model of the 18-foot (5.49-meter) wing, except that the fabric of the wing was not scaled to give the correct canopy membrane flexibility.

A comparison of the data from the 5-foot (1.52-meter) and the 18-foot (5.49-meter) wings is presented in figure 11. The data from the two wings were not identical but the curves have the same character and show the same general level of force and moment coefficients. As may be seen, the smaller wing remained inflated to a lower angle of attack and had a slightly higher value of maximum lift that occurred at a lower angle of attack. These differences are probably due to greater stiffness (relative to its size) of the canopy of the smaller wing. It is interesting to note that, even though there were differences in lift and drag, the lift-drag ratios of the two wings were about the same at

angles of attack above 30°. The wings also exhibited similar stability characteristics.

Lateral Stability and Control

Because the two-balance system was not instrumented to read lateral forces and moments, the lateral data were taken using the full-scale tunnel scale-balance system. The lateral tests were limited to a maximum angle of attack of 70° because of large constant amplitude oscillations of the model when it was sideslipped and were limited in angle of sideslip to ±10° because the wing usually collapsed at sideslip angles slightly above these values, particularly at the lower angles of attack.

The variation and repeatability of the static lateral coefficients of the all-flexible parawing with angle of sideslip for the test angle-of-attack range are shown in figure 12. The solid symbols indicate repeat data. In general, the data show relatively good agreement in trend but show considerable variation in magnitude. These data are summarized in figure 13 in the form of the stability derivatives C_{Y_β}, C_{n_β}, and C_{l_β} with angle of attack. The data were obtained by estimating the average slope of the coefficients through $\beta = 0°$. Because of the nonlinearity of the data, especially at angles of attack of 40° and above, the stability derivatives are only generally indicative of the characteristics of the model. As may be seen, the model had positive values of directional stability $\left(+C_{n_\beta}\right)$ and positive effective dihedral $\left(-C_{l_\beta}\right)$ that decreased with increasing angle of attack and became zero at an angle of attack of about 35°. In the angle-of-attack range from 35° to 45° the parawing was directionally unstable and had negative effective dihedral. These unstable characteristics are a result of the change in sign of the side-force derivative, C_{Y_β}, since this parameter multiplied by its moment arm contributes significantly to the directional stability and effective dihedral characteristics. At the higher angles of attack, the model was again stable and had positive effective dihedral.

It has been suggested that differential deflection of the wing tips (by reeling in and letting out on the tip suspension lines) might be a method of controlling the all-flexible parawing laterally. Data showing the effect of differential tip-line lengths of ±2 and ±4 inches (±0.05 and ±0.10 meter) on the lateral characteristics of the model are presented in figure 14 and are summarized in figures 15 and 16. The variation of the lateral coefficients with sideslip for the model with controls deflected indicates that at an angle of attack of 30° the controls were effective over the test sideslip range. (See fig. 14.) At angles of attack of 35° and above, the model stalled, and there was little consistency in the forces and moments produced by control deflection over the sideslip range. Even though there was nonlinearity in these data with angle of sideslip, the static lateral forces and moments resulting from right to left control are fairly symmetrical when measured at $\beta = 0°$ for the angle-of-attack range investigated. (See fig. 15.) The difference between the right and left control data of figure 15, divided by 2 to give average control characteristics for the system, is shown in figure 16 as the incremental lateral forces and moments produced by a right-wing-down control. For this configuration,

positive (right) rolling moments and negative (left) yawing moments are developed over most of the angle-of-attack range. Since a right-wing-down control produces positive rolling moments, the control system seems to be acting more like a center-of-gravity shift type of control than a conventional aileron type of control.

SUMMARY OF RESULTS

The results of the full-scale-tunnel investigation of the performance and the static stability and control characteristics of the 18-foot (5.49-meter) all-flexible parawing tested may be summarized as follows:

1. The model had a maximum value of lift-drag ratio of about 2.0 and had longitudinally stable trim points over a lift-drag range from about 2.0 to 1.5.

2. The all-flexible parawing was longitudinally stable at angles of attack from about 30° to 40°. At angles of attack above 40°, there was a destabilizing break in the pitching-moment curve and the model was unstable over the remainder of the test angle-of-attack range (up to 100°). As the angle of attack was decreased below about 30°, the nose portion of the wing collapsed, and the entire wing collapsed at an angle of attack near 28°. The wing, however, could be reinflated by increasing the angle of attack.

3. The model was directionally stable and had positive effective dihedral over most of the test angle-of-attack range but was directionally unstable and had negative effective dihedral at angles of attack from about 35° to 45°.

4. Differential deflection of the wing tips for lateral control produced positive rolling moments and negative yawing moments over most of the test angle-of-attack range when the lines were changed in a direction to lower the right wing tip. This is the result that would be expected from a center-of-gravity shift type of control.

Langley Research Center,
National Aeronautics and Space Administration,
Langley Station, Hampton, Va., September 13, 1966,
124-07-03-06-23.

REFERENCES

1. Mechtly, E. A.: The International System of Units – Physical Constants and Conversion Factors. NASA SP-7012, 1964.

2. DeFrance, Smith J.: The N.A.C.A. Full-Scale Wind Tunnel. NACA Rept. 459, 1933.

TABLE I.- SUSPENSION-LINE SPACING

Line	Location along leading edge (a)	Line	Location along keel (a)
L-1 and R-1	38.25 in. (0.97 m)	K-1	27.0 in. (0.69 m)
L-2 and R-2	72.0 in. (1.83 m)	K-2	45.0 in. (1.14 m)
L-3 and R-3	108.0 in. (2.74 m)	K-3	63.0 in. (1.60 m)
L-4 and R-4	144.0 in. (3.66 m)	K-4	81.0 in. (2.06 m)
L-5 and R-5	180.0 in. (4.57 m)	K-5	99.0 in. (2.51 m)
L-6 and R-6	216.0 in. (5.49 m)	K-6	117.0 in. (2.97 m)
		K-7	139.5 in. (3.54 m)
		K-8	162.0 in. (4.11 m)
		K-9	180.0 in. (4.57 m)
		K-10	198.0 in. (5.03 m)
		K-11	216.0 in. (5.49 m)

[a]From theoretical apex (see fig. 1).

TABLE II.- LINE RIGGING OF THE 18-FOOT (5.49-METER)

PARAWING (SEE FIG. 1)

Line	Length		Line	Length	
	Basic	Modified		Basic	Modified
L-1 and R-1	288.0 in. (7.32 m)	295.7 in. (7.51 m)	K-1	279.0 in (7.09 m)	292.5 in. (7.43 m)
L-2 and R-2	276.8 in (7.03 m)	281.0 in. (7.14 m)	K-2	284.0 in. (7.21 m)	291.6 in. (7.41 m)
L-3 and R-3	267.3 in. (6.79 m)	270.4 in. (6.87 m)	K-3	286.2 in. (7.27 m)	289.7 in. (7.36 m)
L-4 and R-4	252.0 in. (6.40 m)	257.9 in. (6.55 m)	K-4	281.7 in. (7.16 m)	288.4 in. (7.33 m)
L-5 and R-5	241.7 in. (6.14 m)	246.7 in. (6.27 m)	K-5	276.3 in. (7.02 m)	284.3 in. (7.22 m)
L-6 and R-6	216.2 in. (5.49 m)	224.2 in. (5.69 m)	K-6	274.5 in. (6.97 m)	280.1 in. (7.11 m)
			K-7	274.5 in. (6.97 m)	276.7 in. (7.03 m)
			K-8	274.5 in. (6.97 m)	272.8 in. (6.93 m)
			K-9	271.3 in. (6.89 m)	267.4 in. (6.79 m)
			K-10	255.0 in. (6.48 m)	259.2 in. (6.58 m)
			K-11	236.3 in. (6.00 m)	238.5 in. (6.06 m)

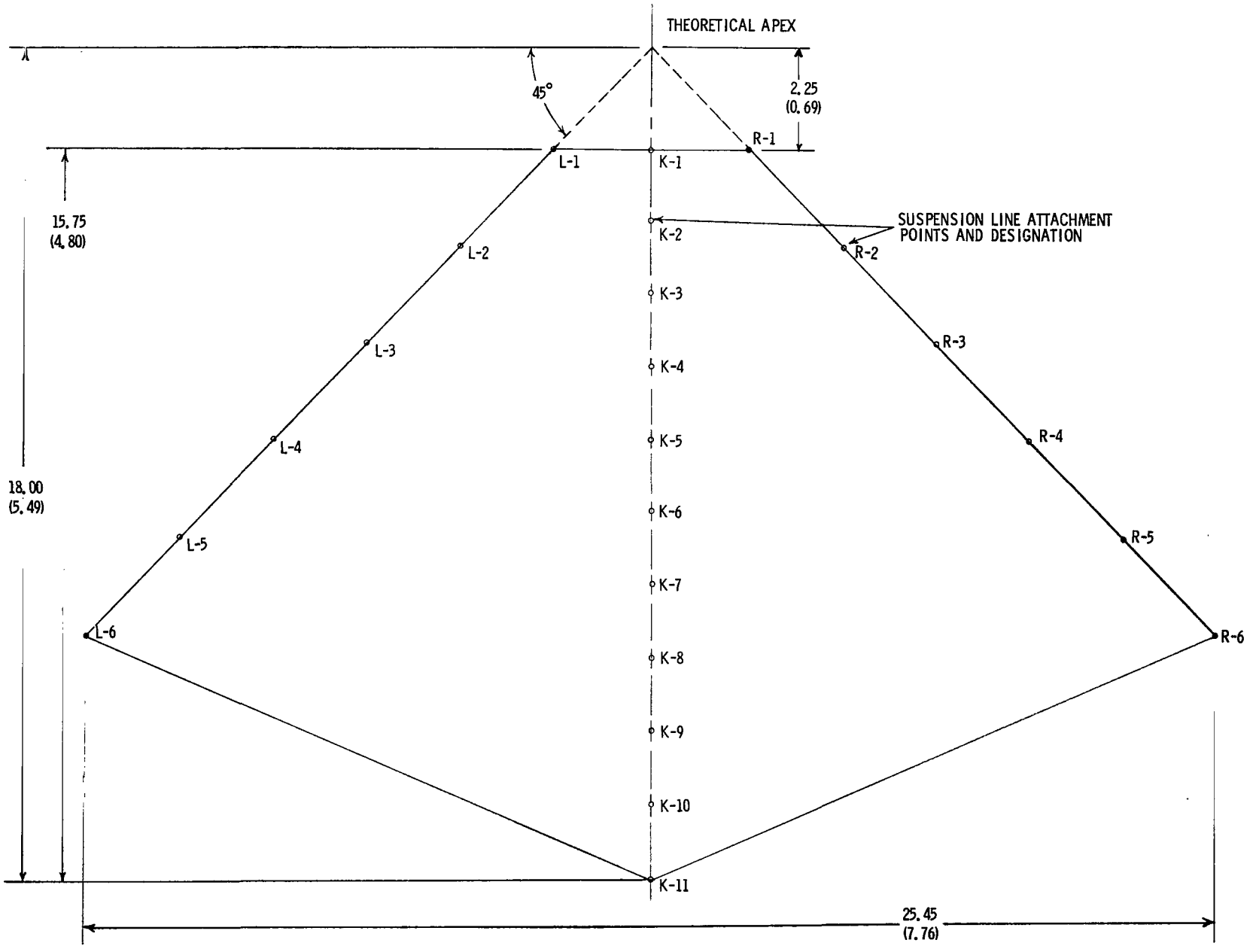

Figure 1.- Flat plan geometry of all-flexible parawing canopy showing suspension-line locations. Linear dimensions are in feet (meters). See table I for line spacing.

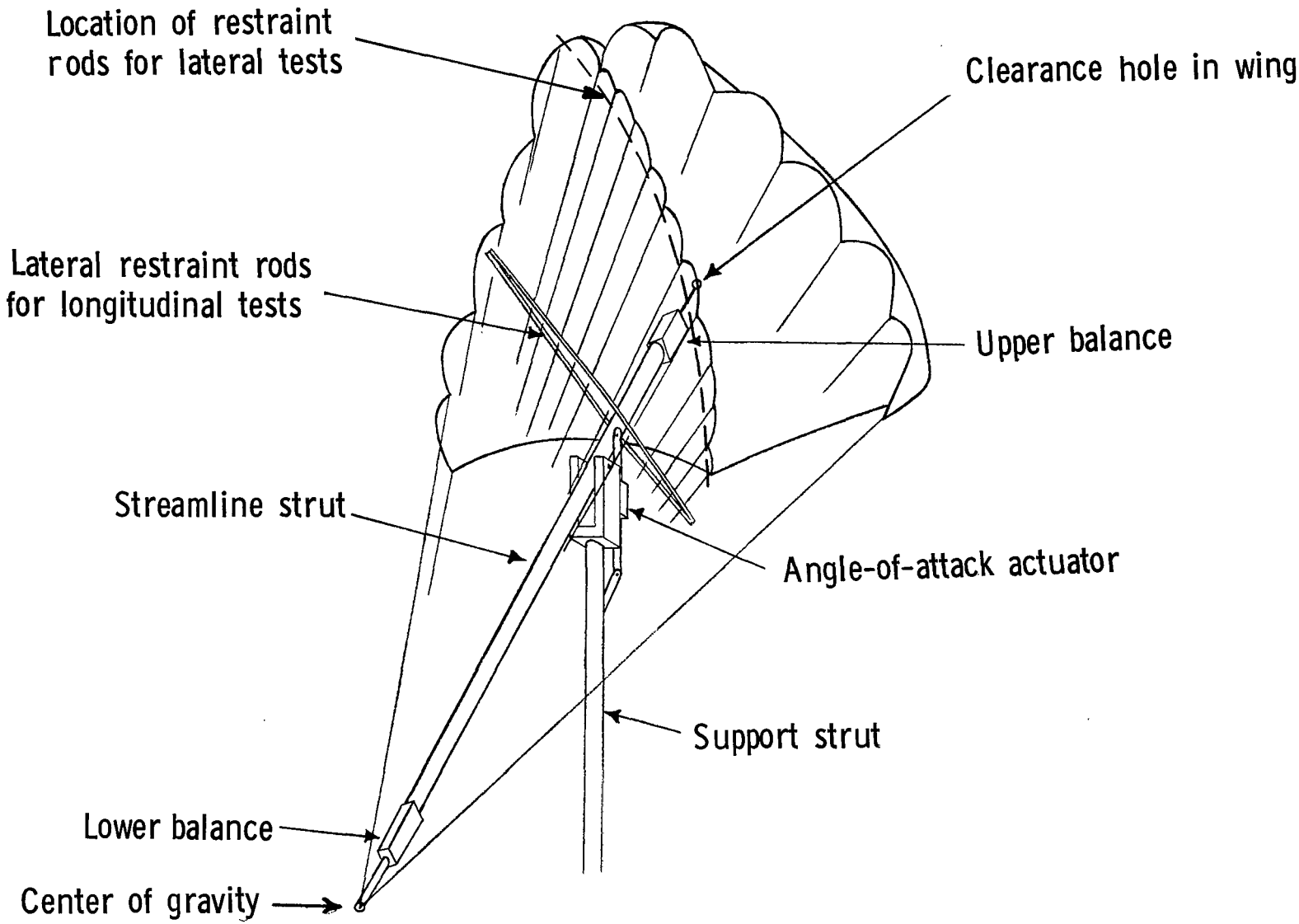

Figure 2.- Sketch showing setup for force testing in Langley full-scale tunnel.

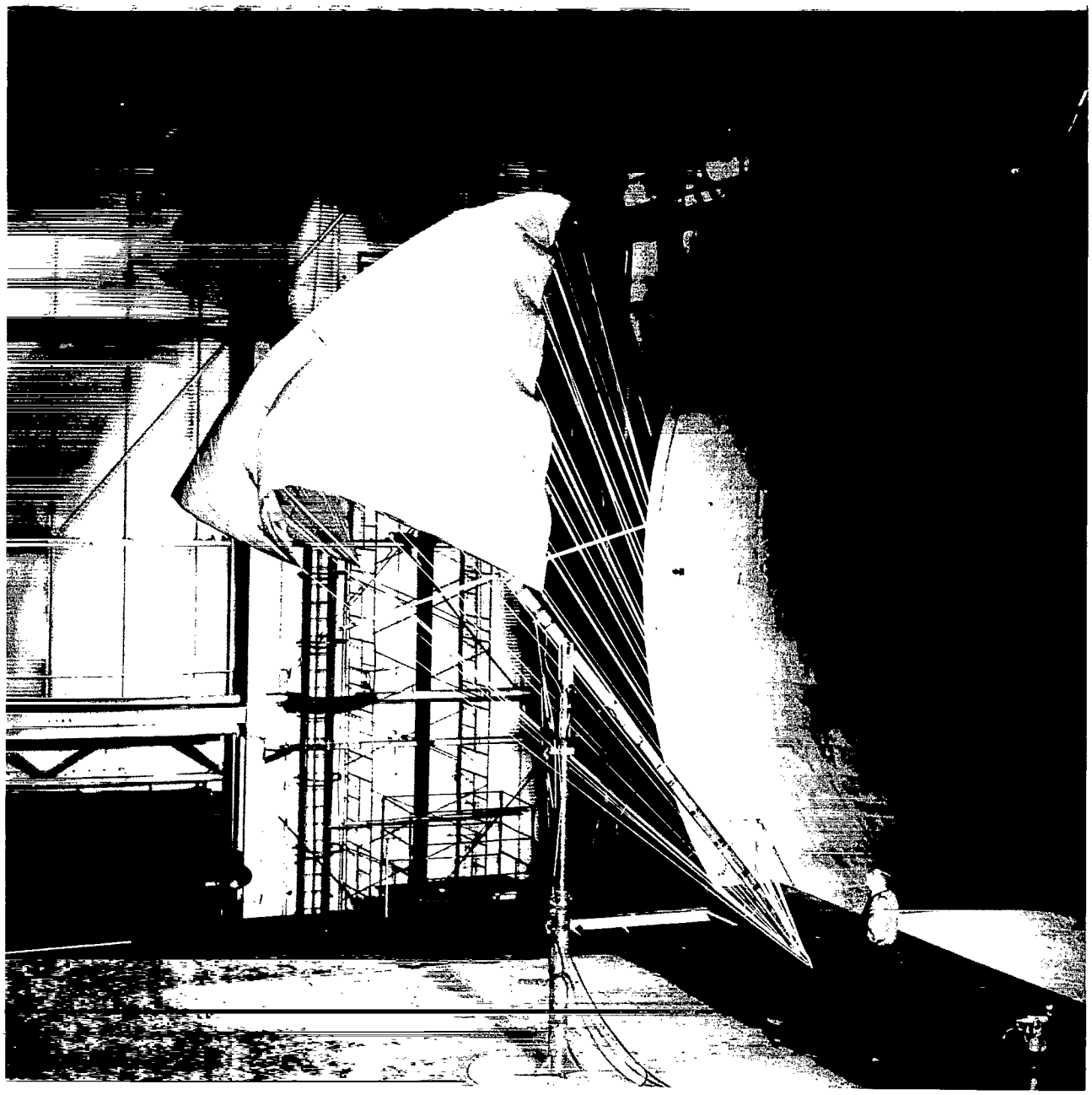

Figure 3.- Photograph of model mounted in Langley full-scale tunnel. L-66-237

$$F_{A,T} = F_{A,l} + F_{A,u}$$

$$F_{N,T} = F_{N,l}$$

$$M_T = M_{Y,u} + F_{A,u}(x)$$

$$C_L = \frac{F_{N,T}}{qS}\cos\alpha + \frac{F_{A,T}}{qS}\sin\alpha$$

$$C_D = \frac{F_{N,T}}{qS}\sin\alpha - \frac{F_{A,T}}{qS}\cos\alpha$$

$$C_m = \frac{M_T}{qSl_k}$$

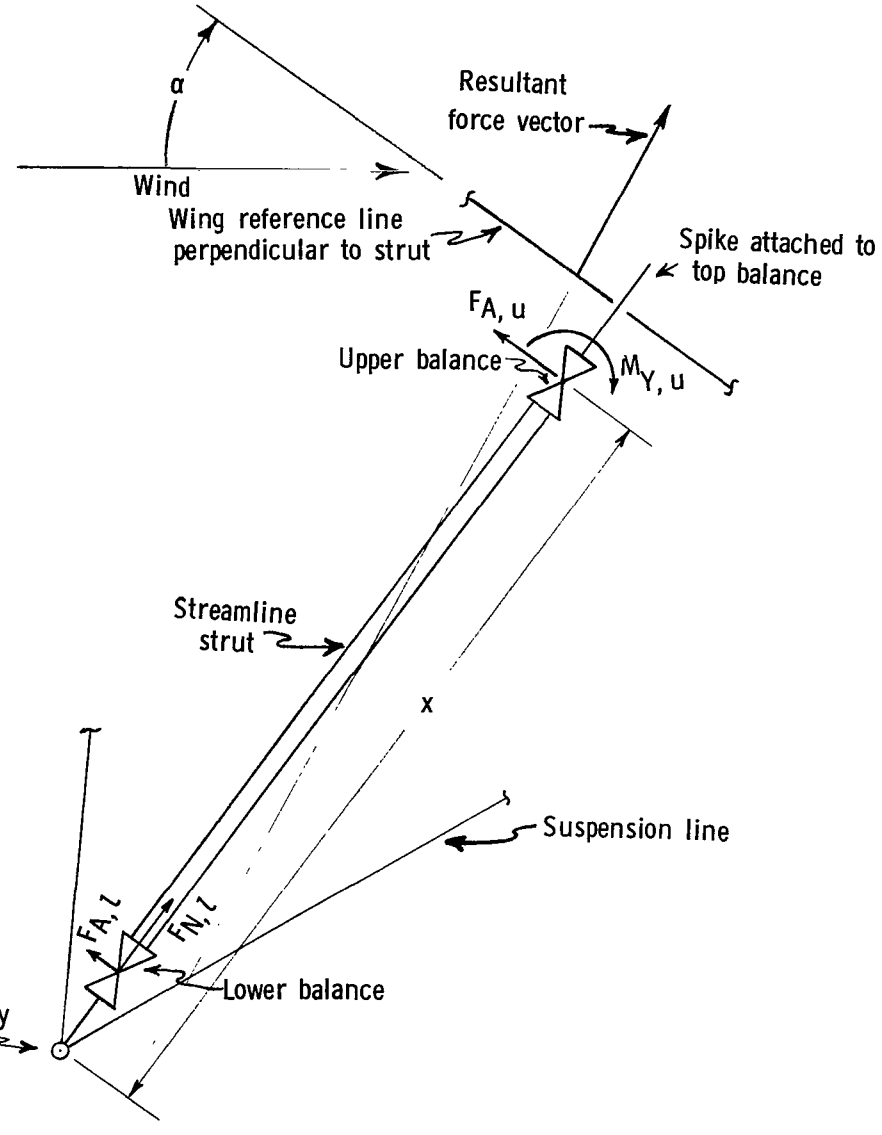

Figure 4.- Sketch showing how forces and moments are measured with two-balance system. Arrows indicate positive direction of forces and moments.

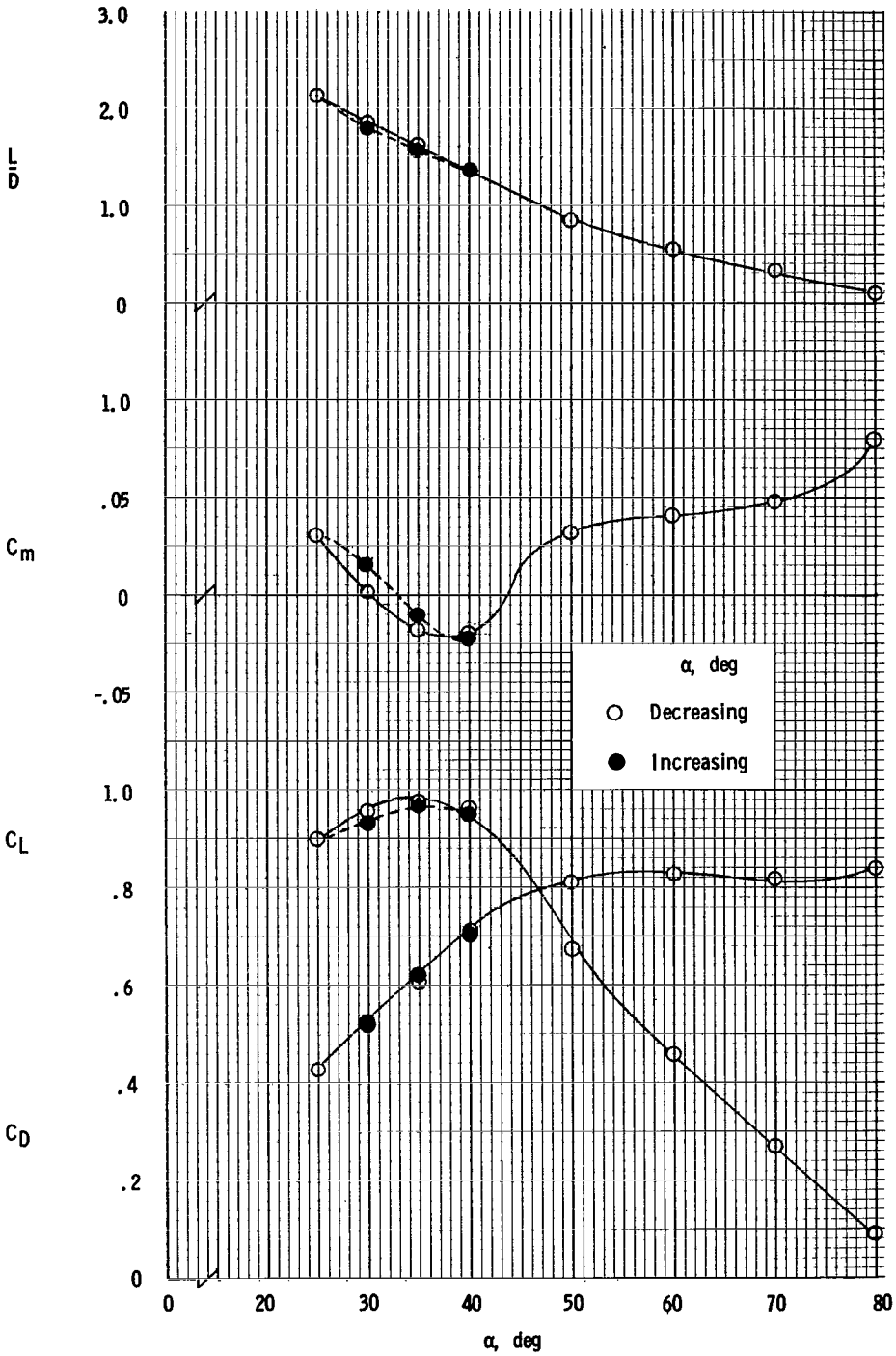

Figure 5.- Effect of direction of variation of angle of attack on static longitudinal characteristics of model with modified rigging. $\beta = 0^{o}$; q = 1.0 lb/sq ft (47.9 newtons/sq meter).

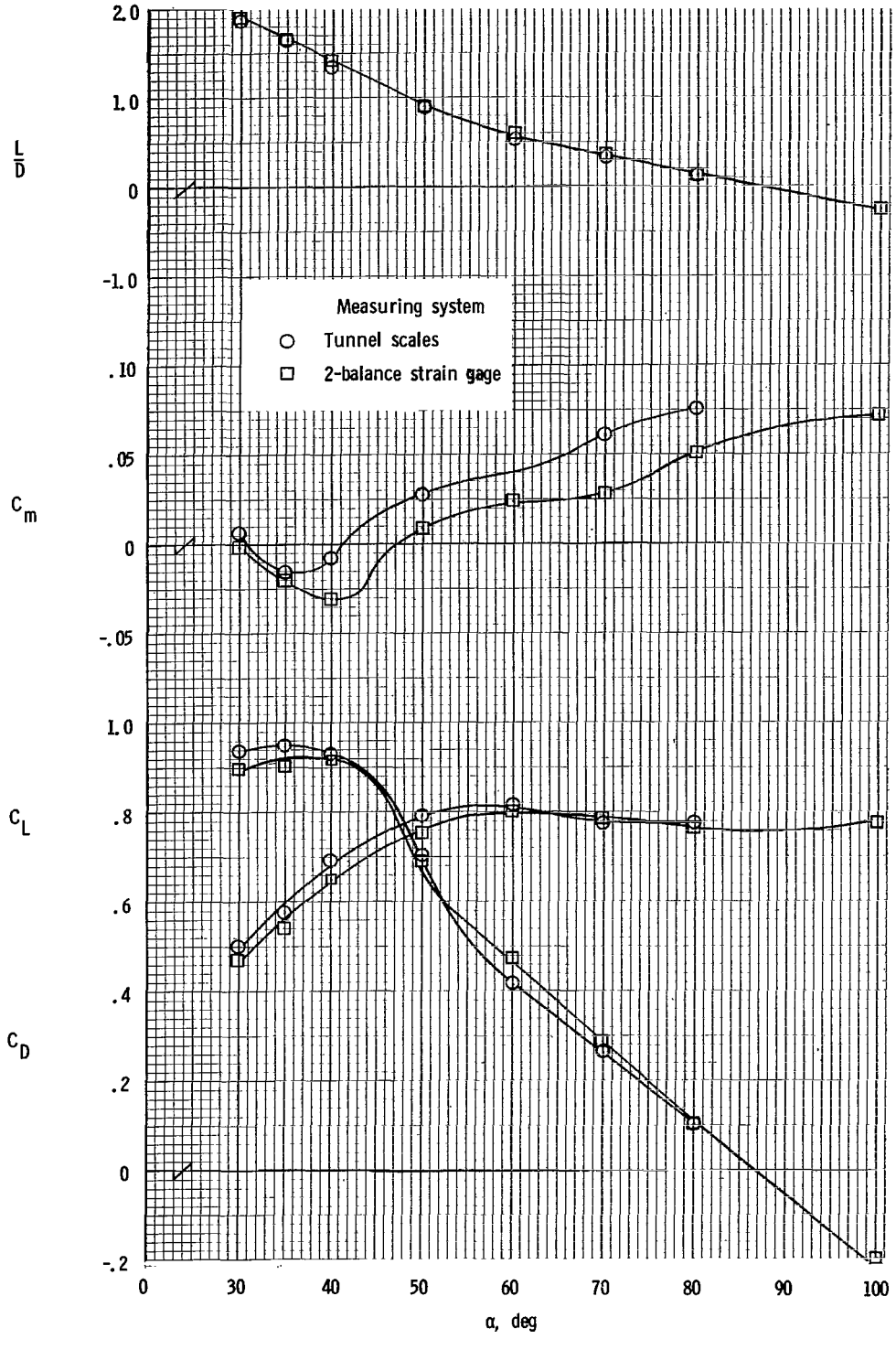

Figure 6.- Comparison of static longitudinal characteristics of model with basic rigging as measured by Langley full-scale tunnel scale system and strain-gage system. $\beta = 0^{o}$; $q = 1.0$ lb/sq ft (47.9 newtons/sq meter).

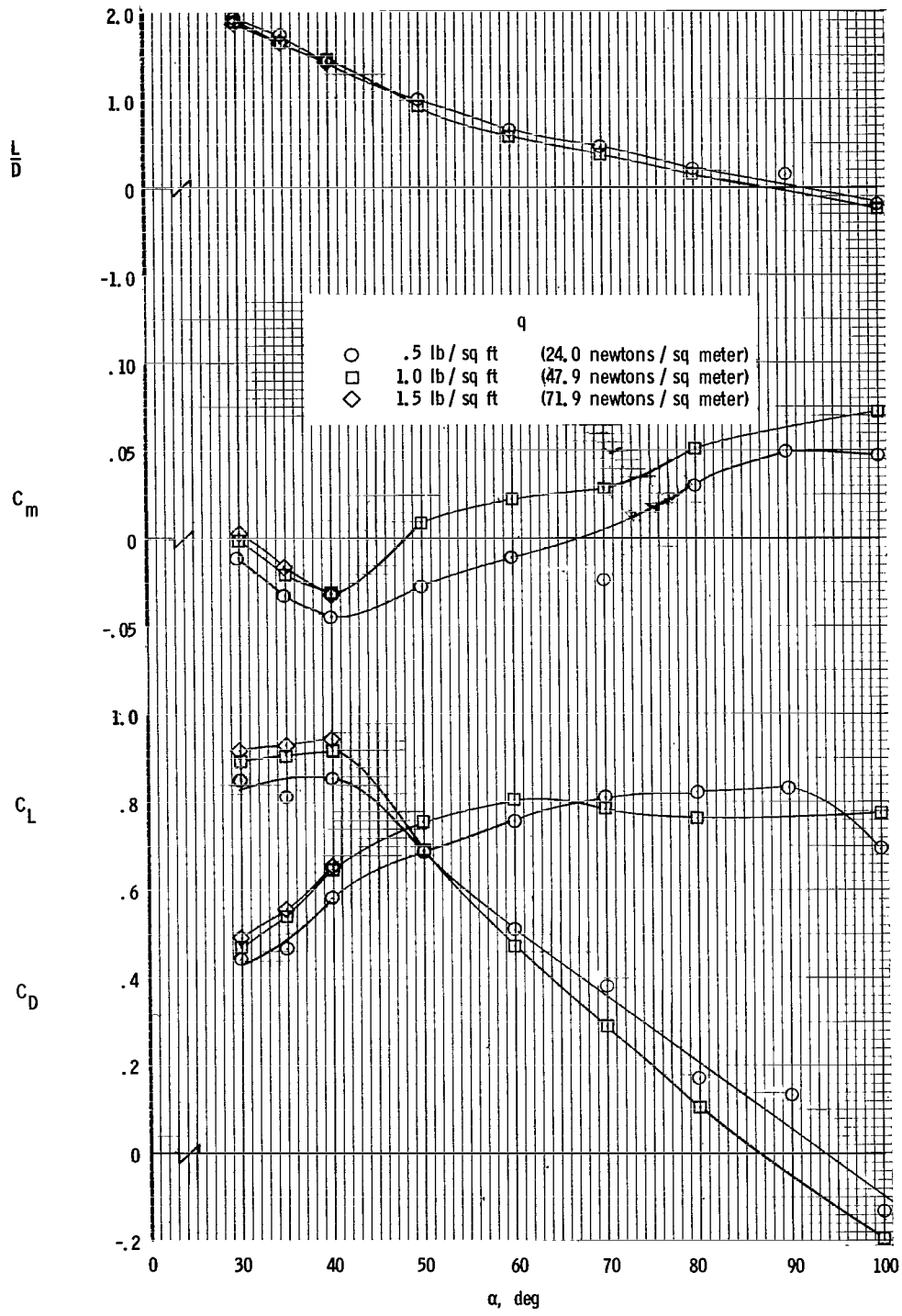

Figure 7.- Static longitudinal characteristics of model with basic rigging. $\beta = 0^{o}$.

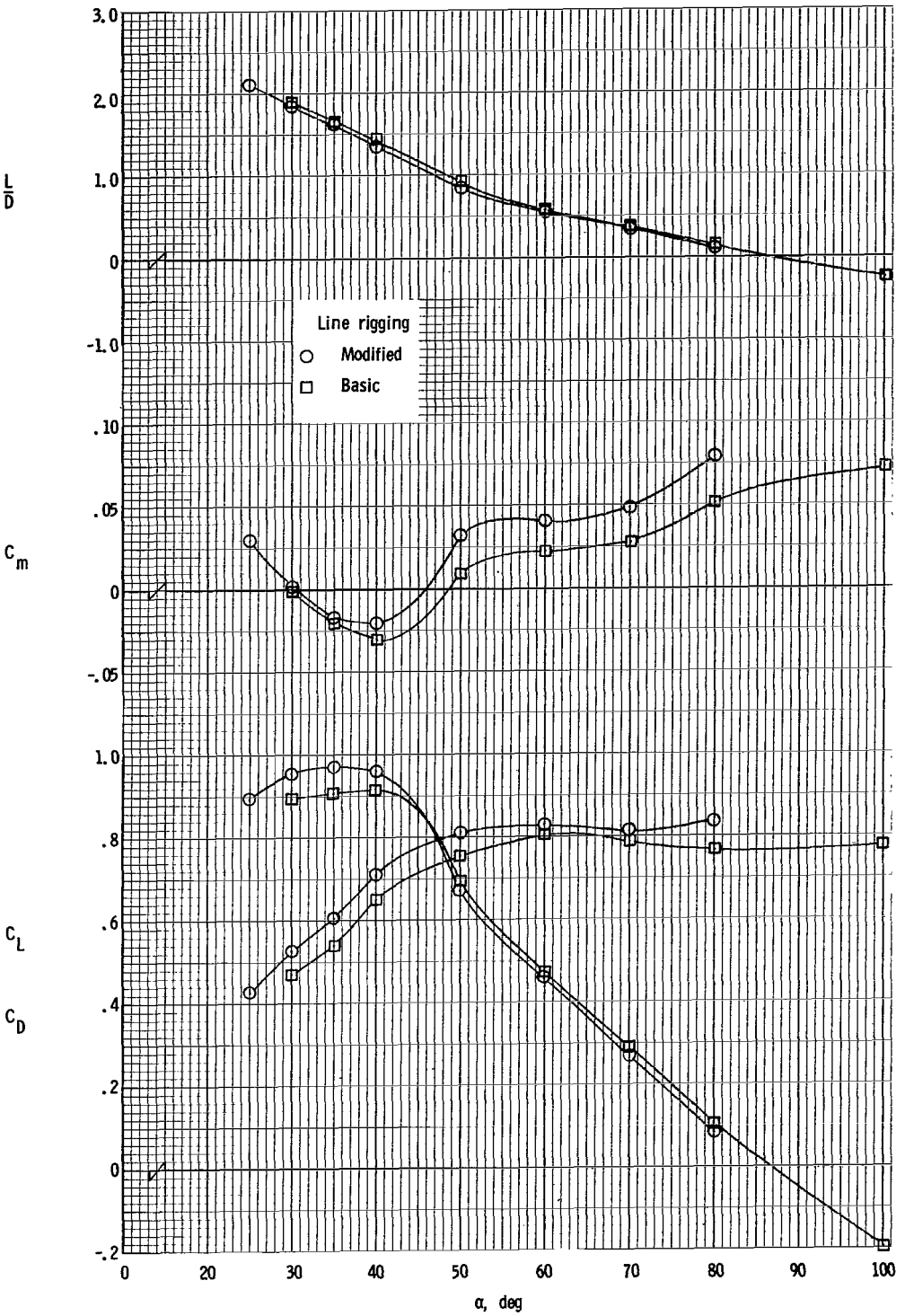

Figure 8.- Effect of suspension-line rigging on static longitudinal characteristics of model. $\beta = 0^0$; $q = 1.0$ lb/sq ft (47.9 newtons/sq meter).

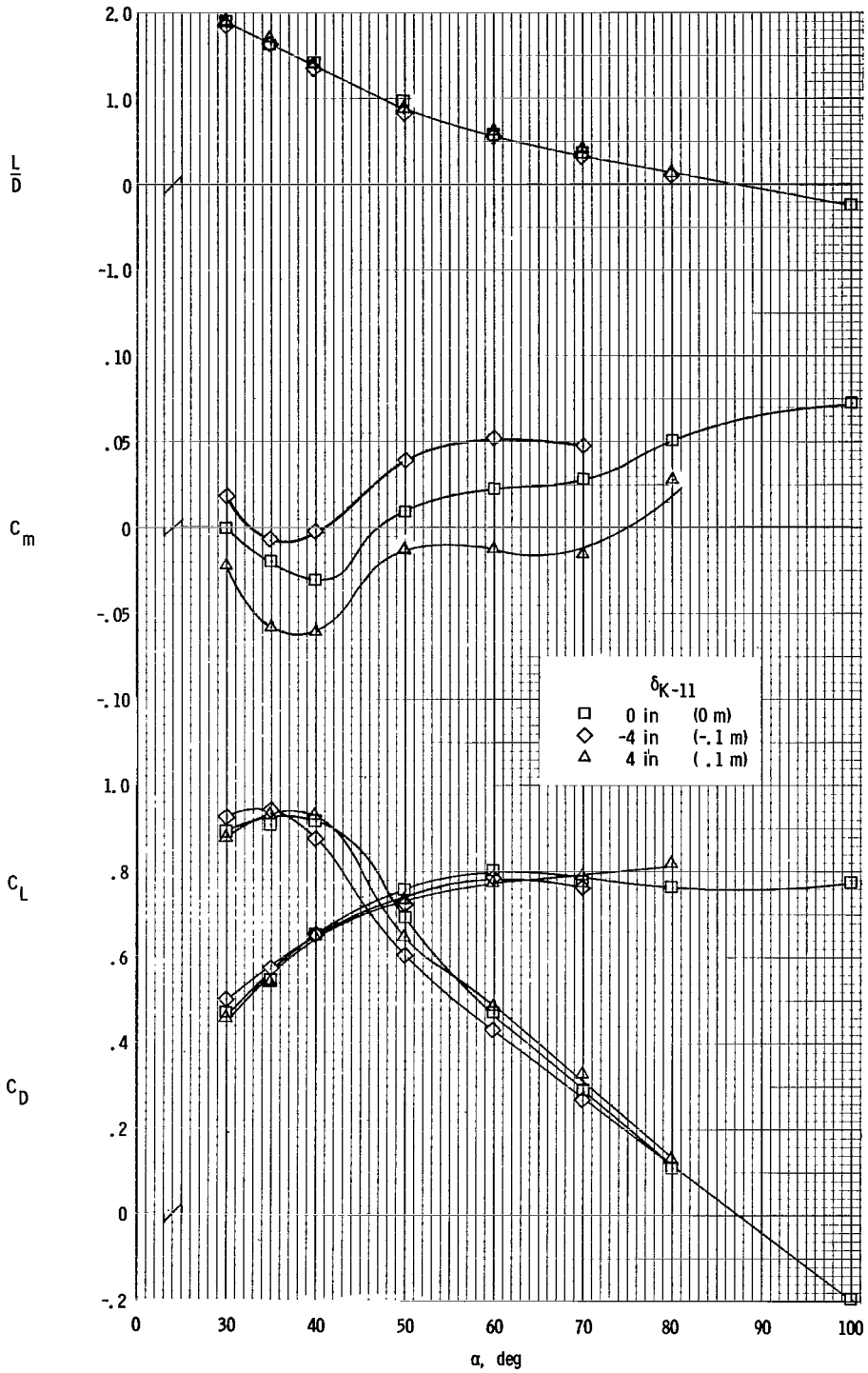

Figure 9.- Effect of changes in length of keel line for pitch control. Basic rigging; $\beta = 0^{o}$; q = 1.0 lb/sq ft (47.9 newtons/sq meter).

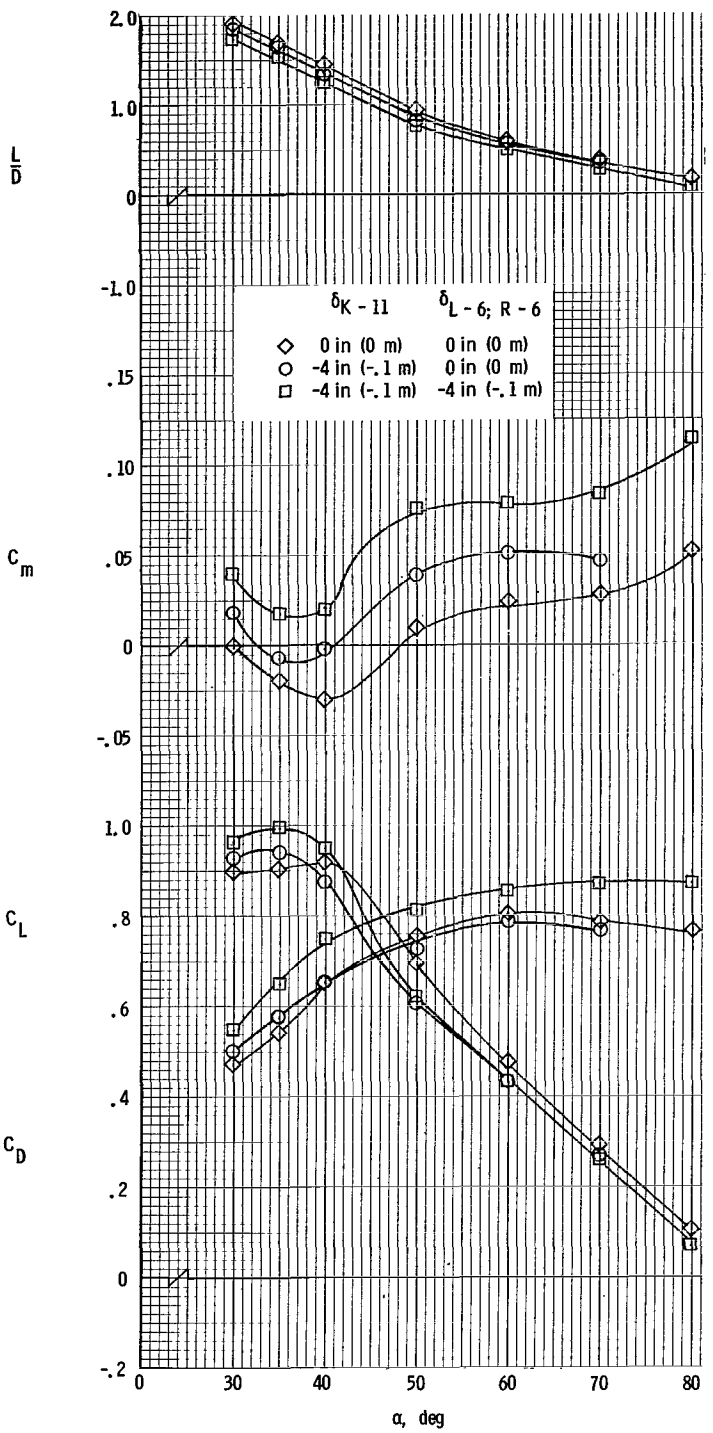

Figure 10.- Comparison of effects of changes of length of keel line with changes in length of keel line plus two wing-tip lines for pitch control with basic rigging. $\beta = 0^o$; q = 1.0 lb/sq ft (47.9 newtons/sq meter).

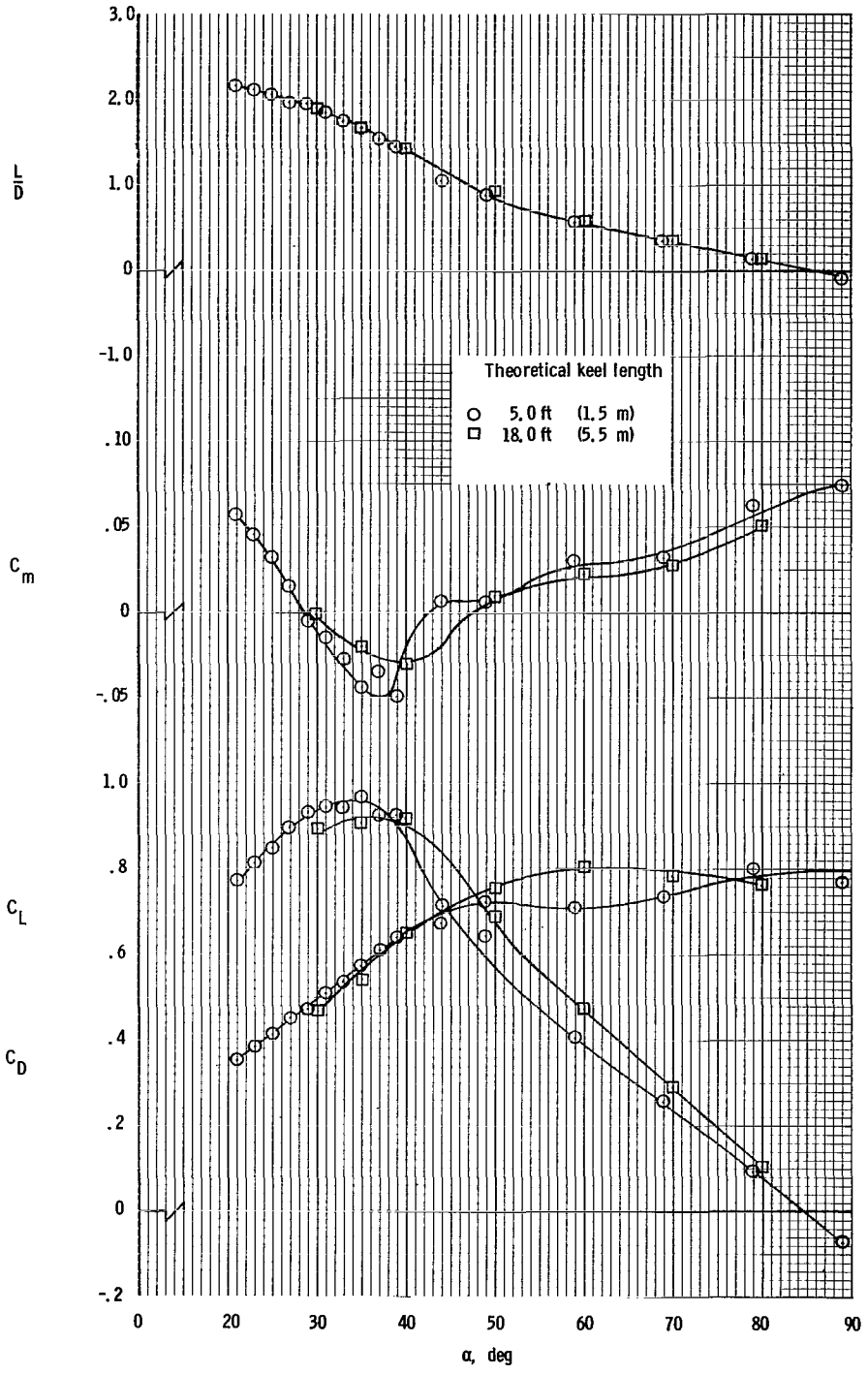

Figure 11.- Comparison of static longitudinal characteristics of 18-foot wing basic rigging with geometrically similar 5-foot wing. $\beta = 0^0$; q = 1.0 lb/sq ft (47.9 newtons/sq meter).

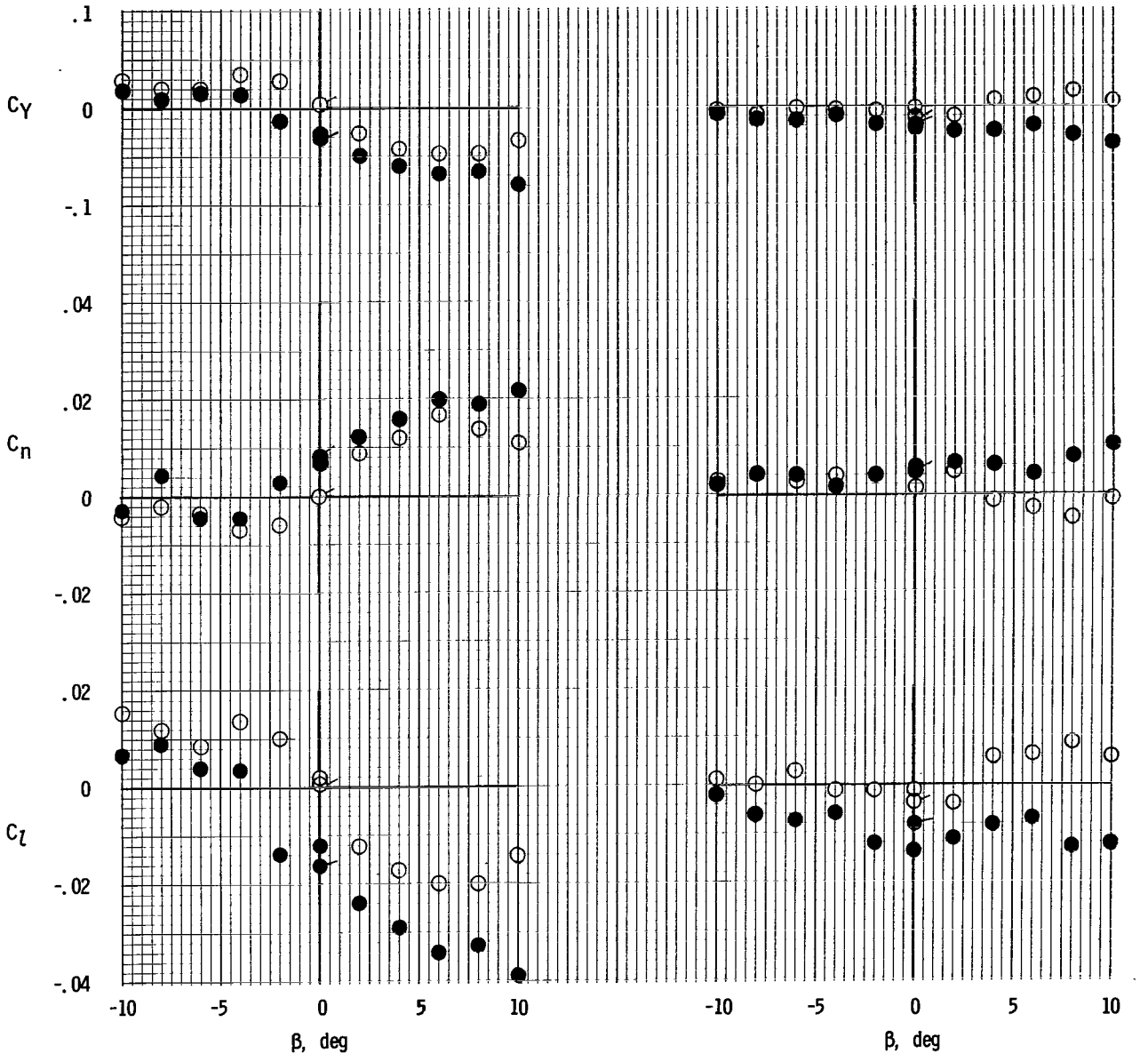

(a) $\alpha = 30^0$.

(b) $\alpha = 35^0$.

Figure 12.- Variation of lateral coefficients with angle of sideslip. Solid symbols indicate repeat data. Flagged symbols indicate repeat point. Basic rigging.

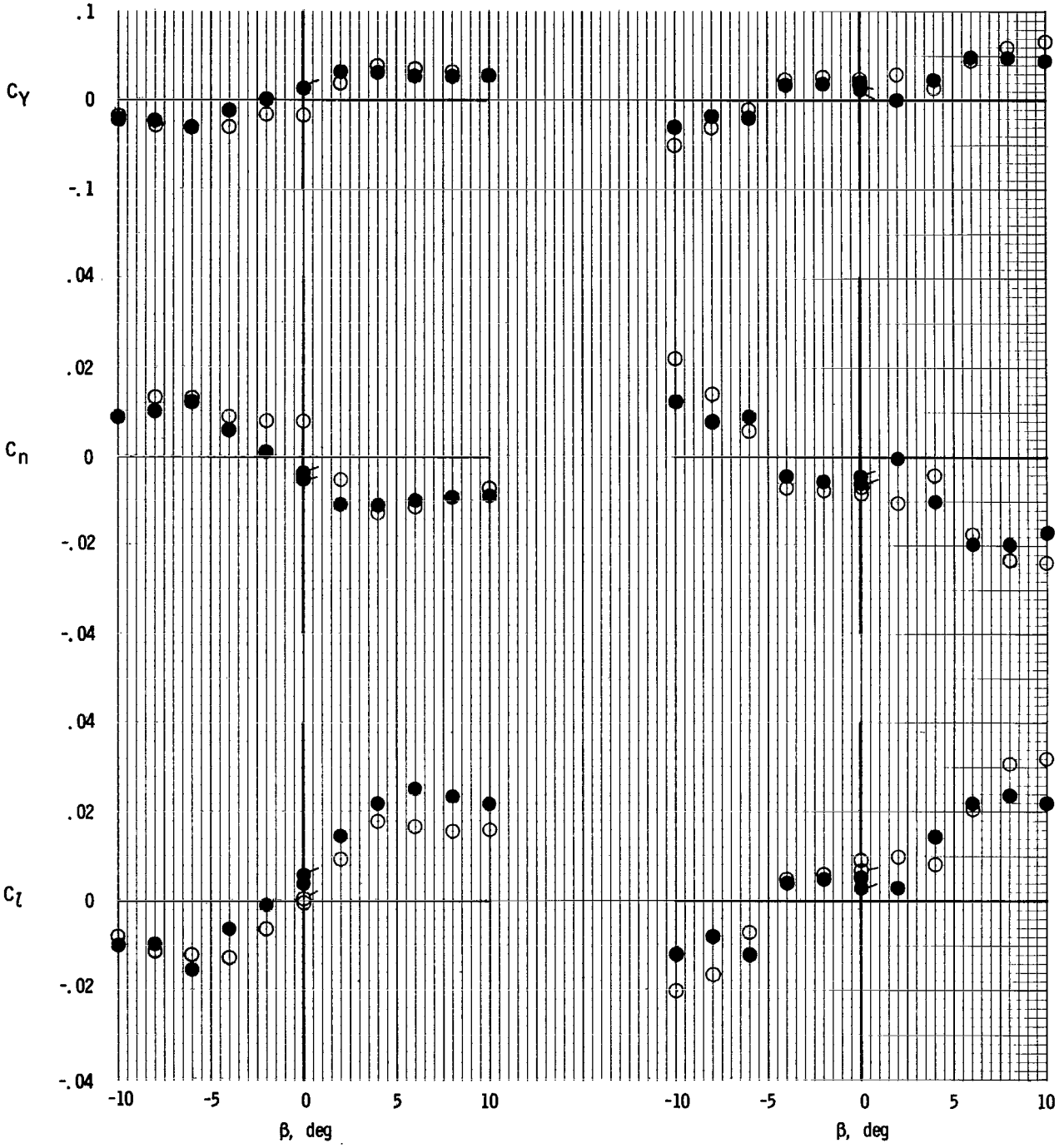

(c) $\alpha = 40^0$.

(d) $\alpha = 45^0$.

Figure 12.- Continued.

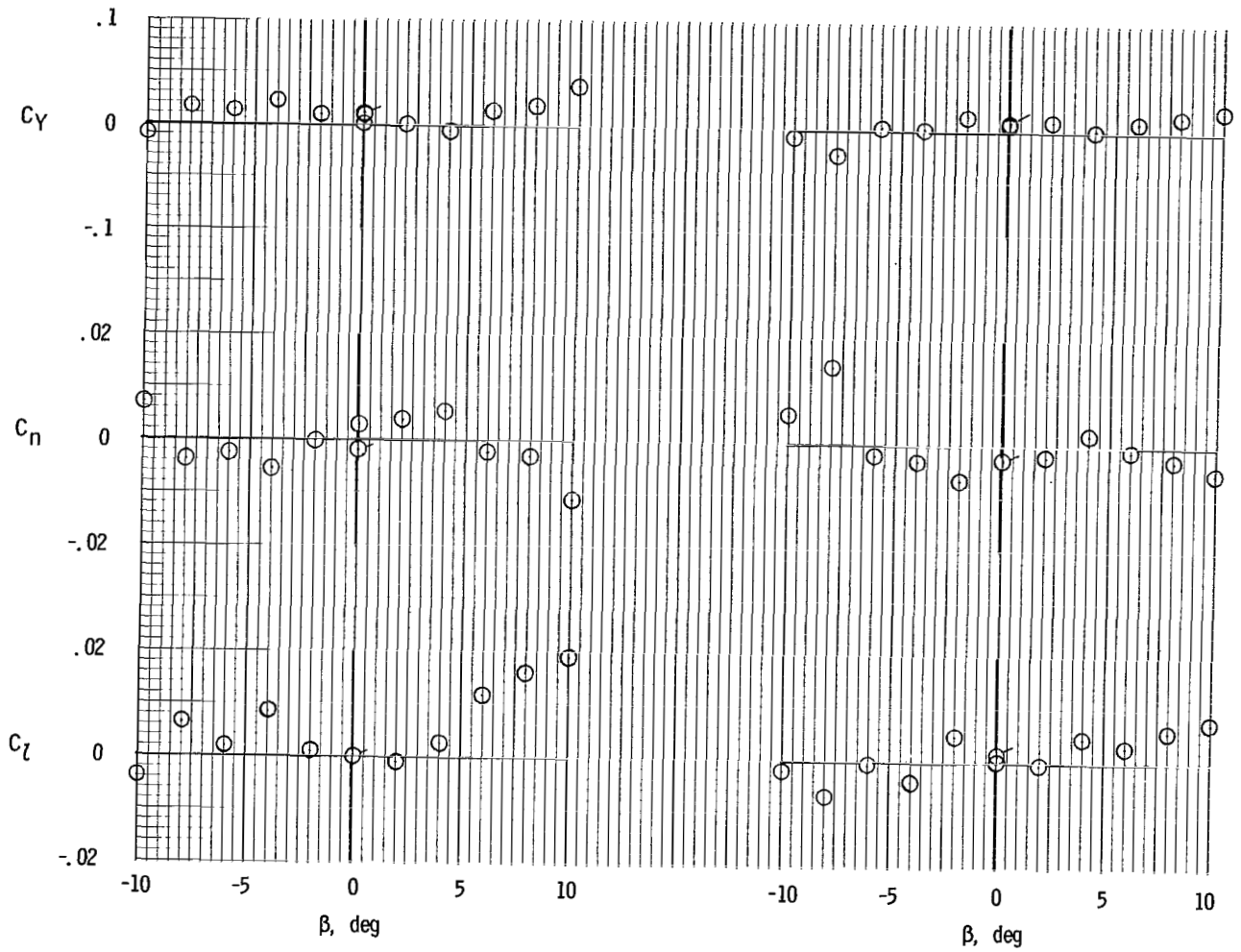

(e) $\alpha = 50^0$.

(f) $\alpha = 70^0$.

Figure 12.- Concluded.

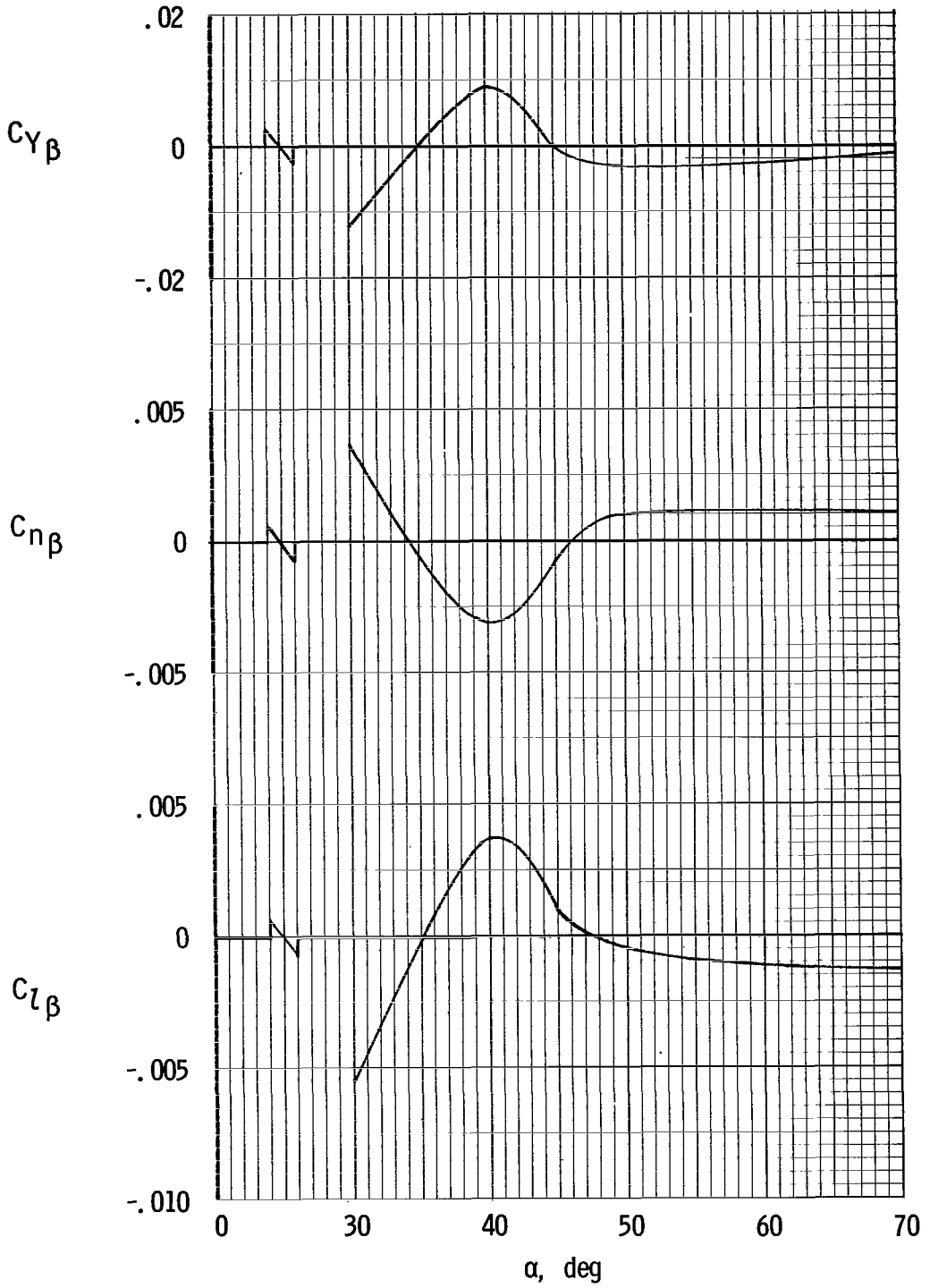

Figure 13.- Lateral stability characteristics of the all-flexible parawing. Basic rigging.

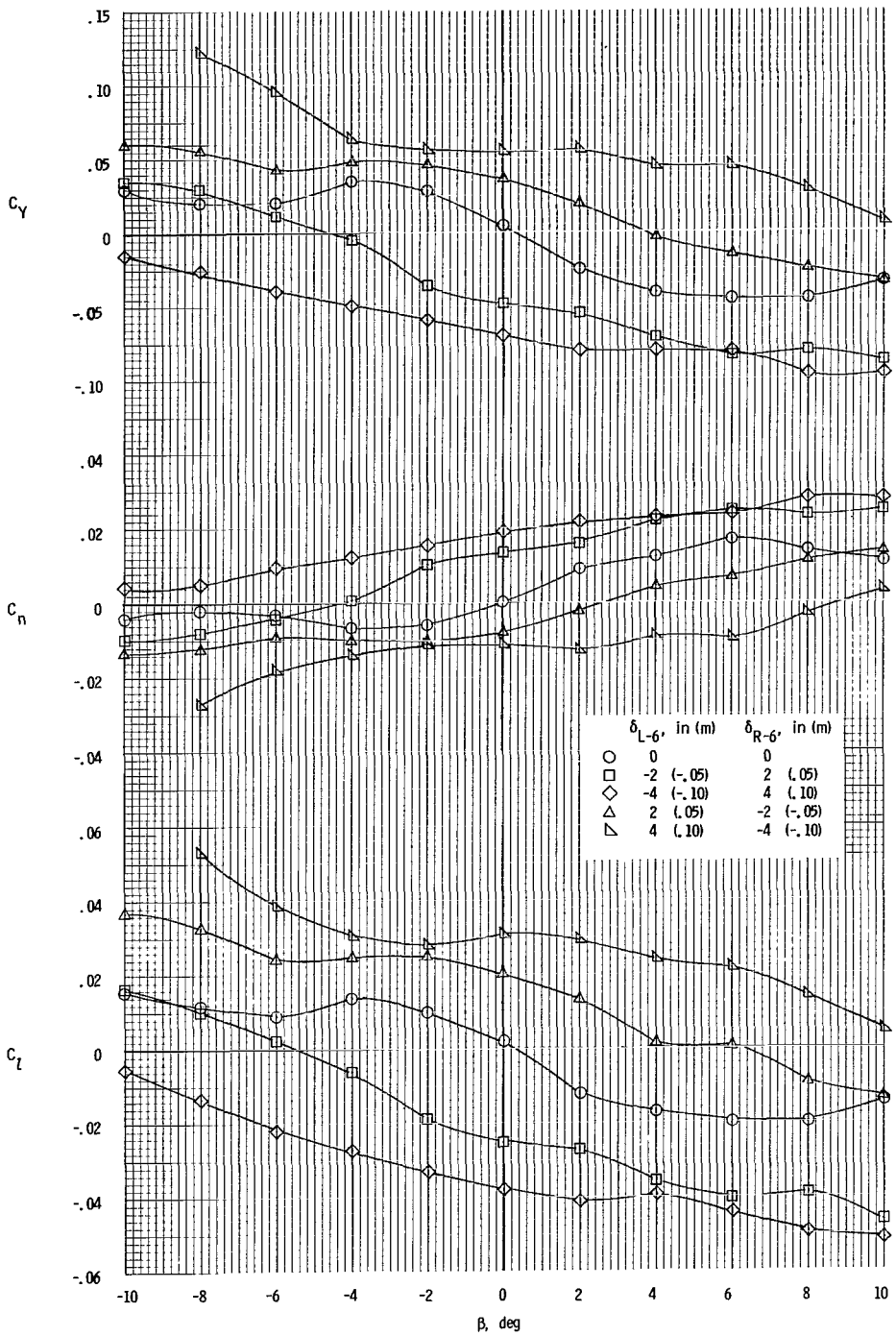

(a) $\alpha = 30^{\circ}$.

Figure 14.- Variation of lateral coefficients of the model with differential wing-tip line deflection at angles of sideslip. Basic rigging.

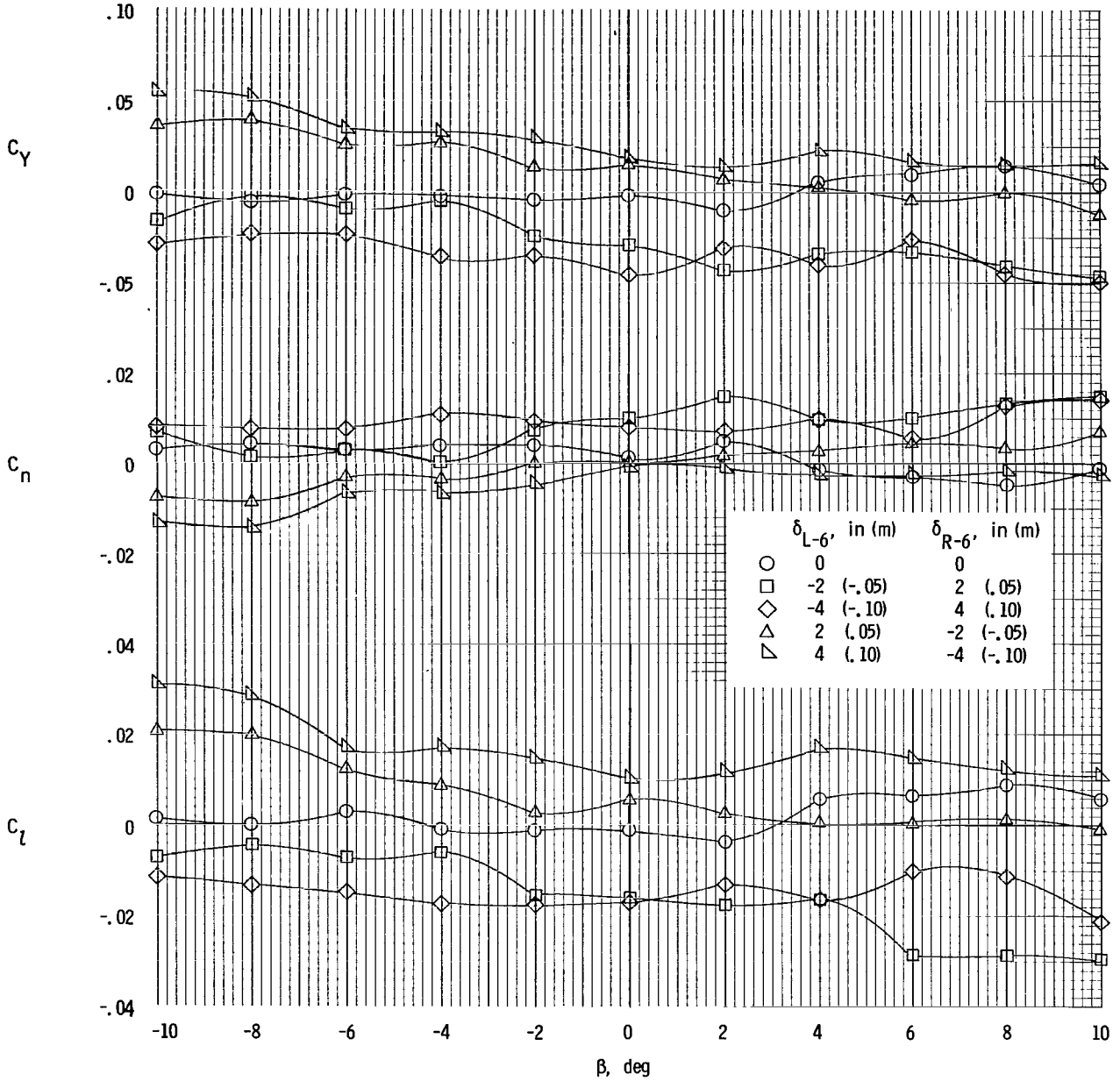

(b) $\alpha = 35^0$.

Figure 14.- Continued.

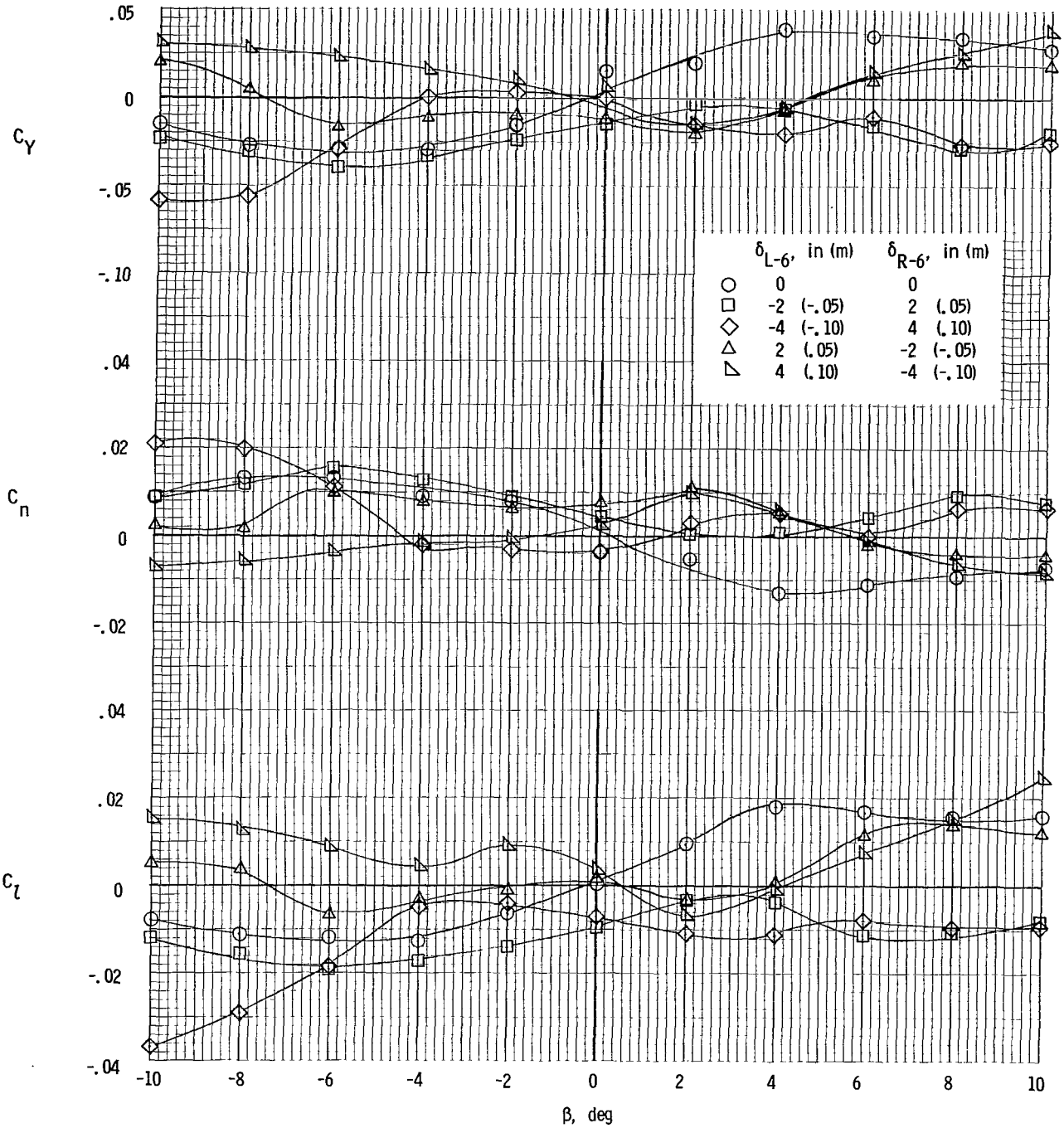

(c) $\alpha = 40^0$.

Figure 14.- Continued.

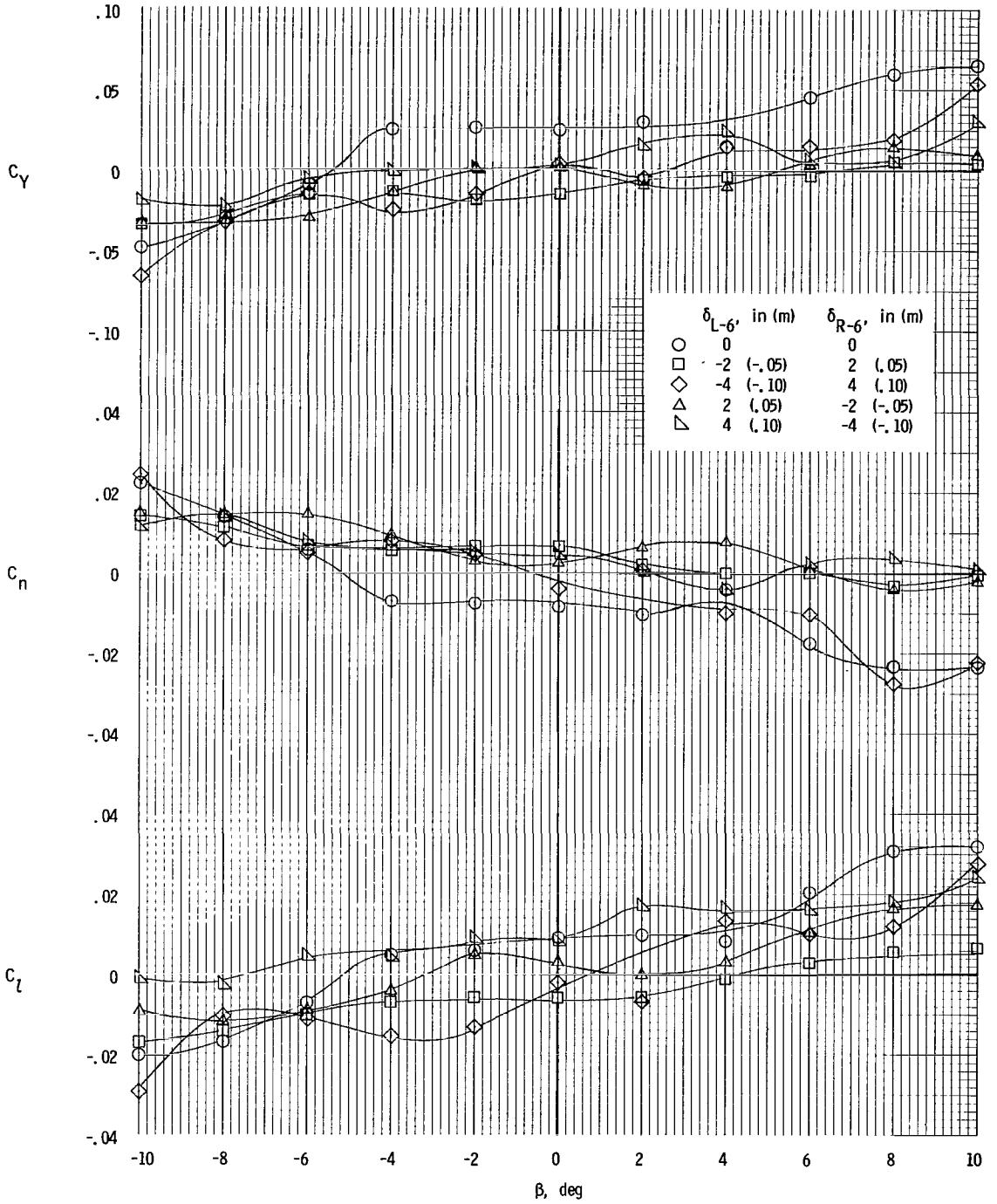

(d) $\alpha = 45^0$.

Figure 14.- Continued.

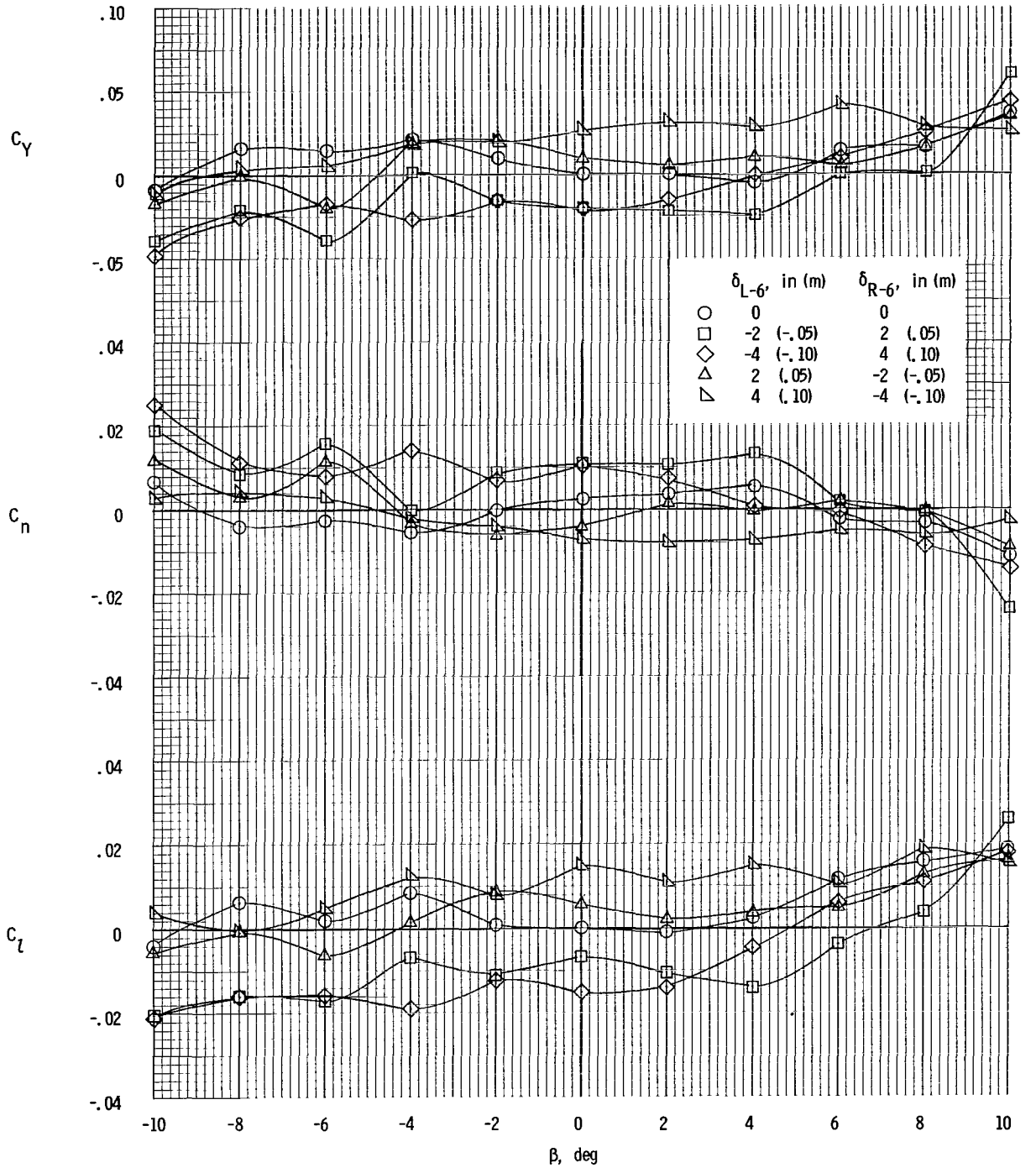

(e) $\alpha = 50^0$.

Figure 14.- Continued.

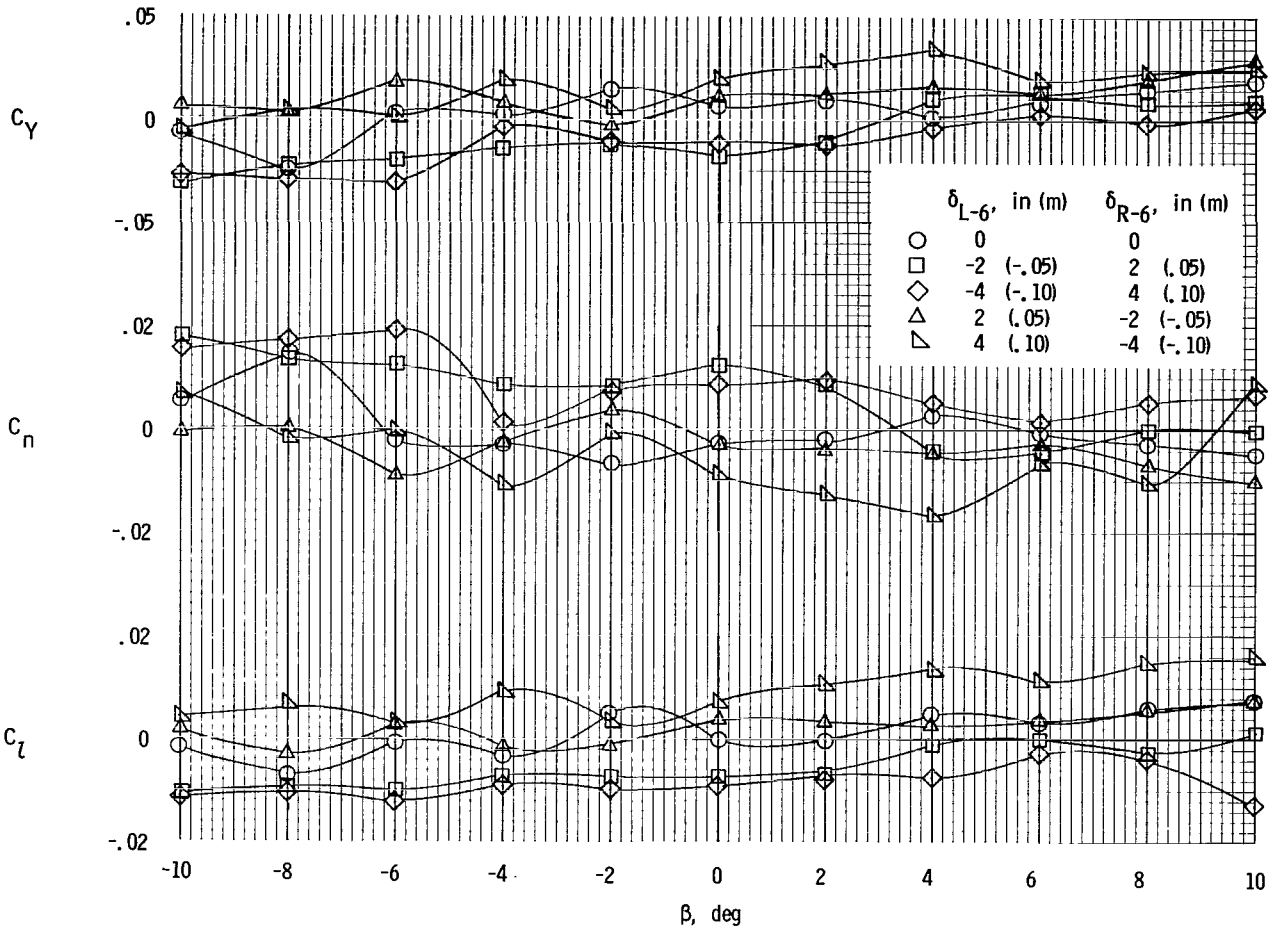

(f) $\alpha = 70^0$.

Figure 14.- Concluded.

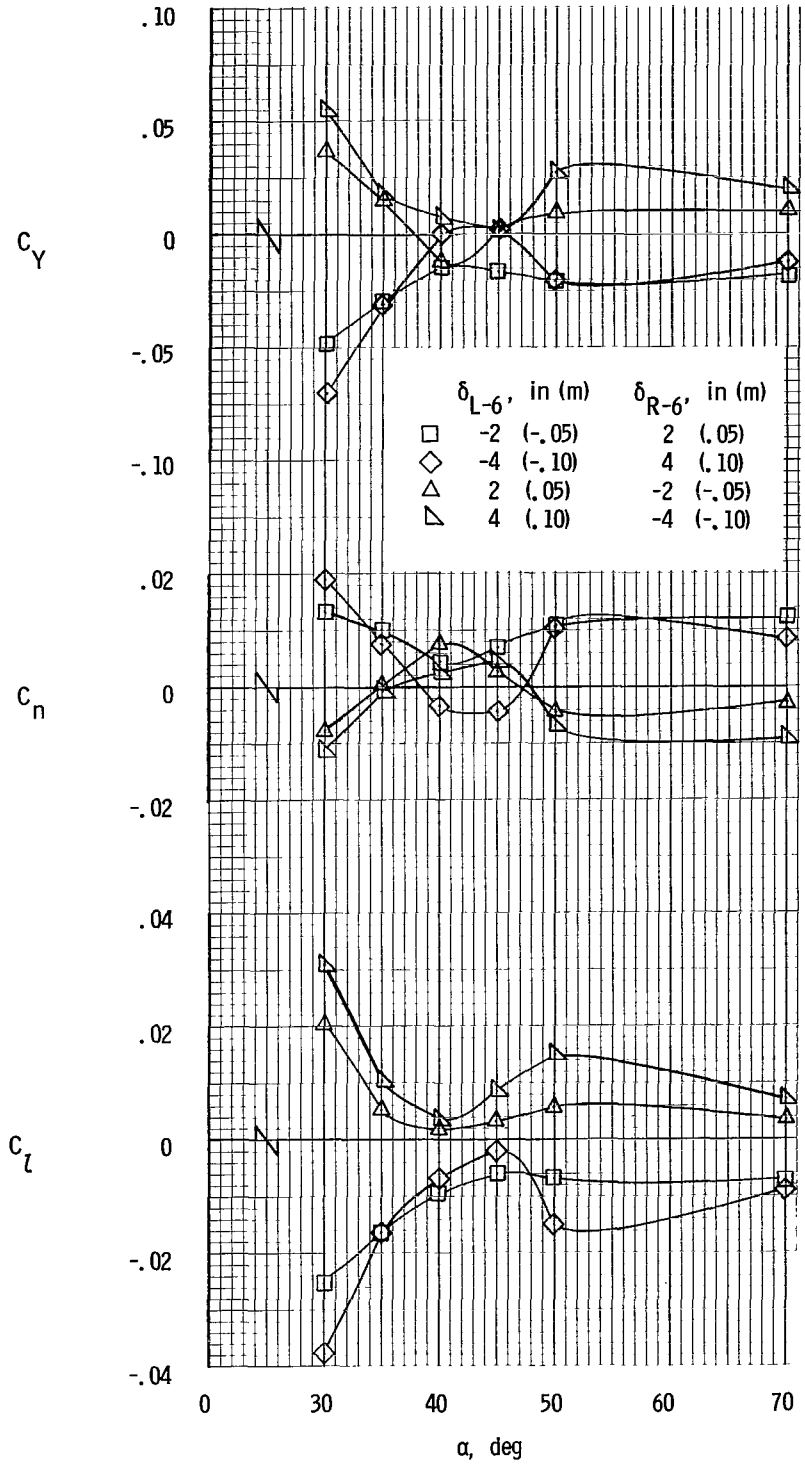

Figure 15.- Effect of differential wing-tip line deflection on the lateral characteristics of the model. Basic rigging. $\beta = 0^{o}$.

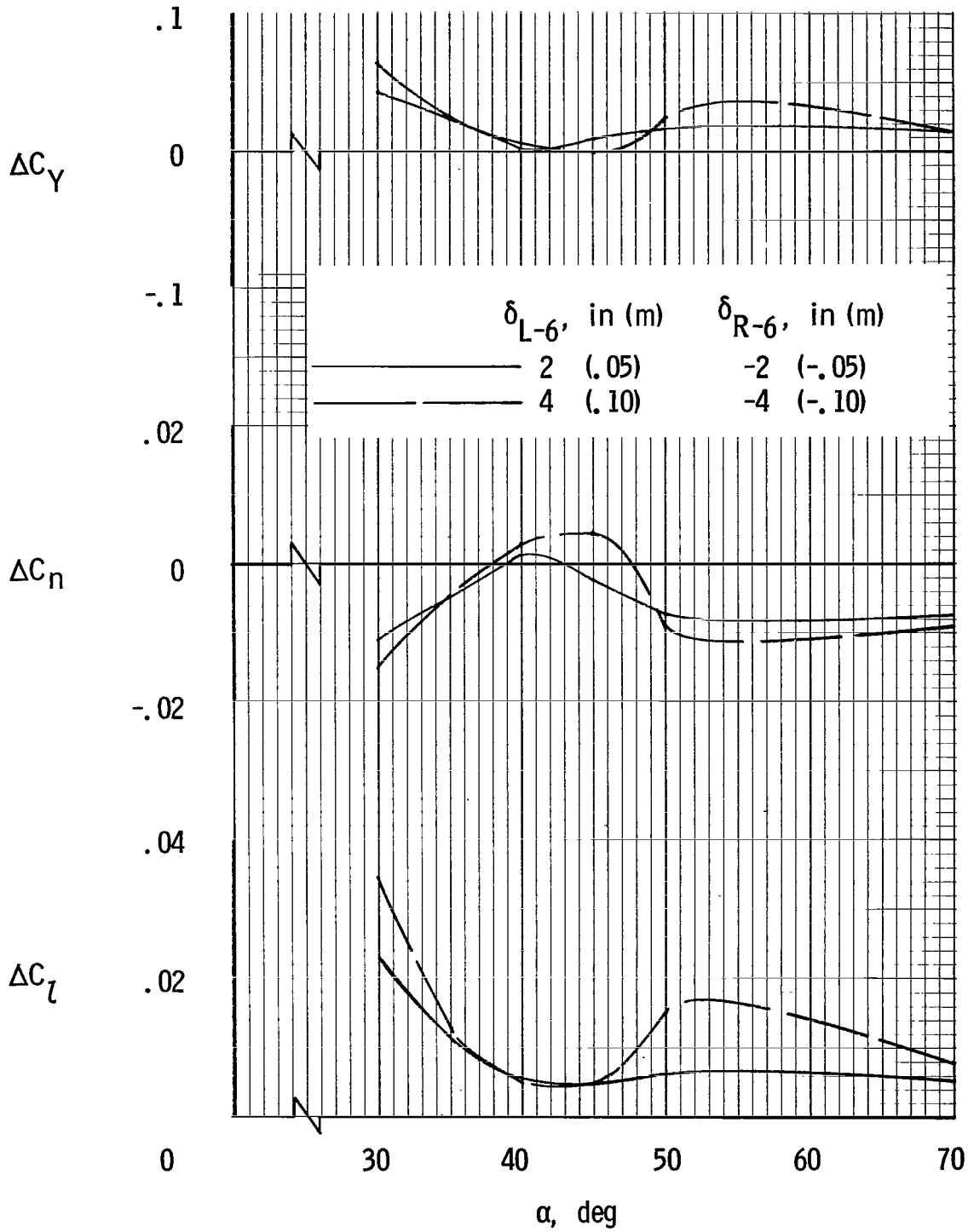

Figure 16.- Average incremental lateral force and moments produced by differential wing-tip deflection. Basic rigging. $\beta = 0^o$.

"The aeronautical and space activities of the United States shall be conducted so as to contribute . . . to the expansion of human knowledge of phenomena in the atmosphere and space. The Administration shall provide for the widest practicable and appropriate dissemination of information concerning its activities and the results thereof."

—NATIONAL AERONAUTICS AND SPACE ACT OF 1958

NASA SCIENTIFIC AND TECHNICAL PUBLICATIONS

TECHNICAL REPORTS: Scientific and technical information considered important, complete, and a lasting contribution to existing knowledge.

TECHNICAL NOTES: Information less broad in scope but nevertheless of importance as a contribution to existing knowledge.

TECHNICAL MEMORANDUMS: Information receiving limited distribution because of preliminary data, security classification, or other reasons.

CONTRACTOR REPORTS: Scientific and technical information generated under a NASA contract or grant and considered an important contribution to existing knowledge.

TECHNICAL TRANSLATIONS: Information published in a foreign language considered to merit NASA distribution in English.

SPECIAL PUBLICATIONS: Information derived from or of value to NASA activities. Publications include conference proceedings, monographs, data compilations, handbooks, sourcebooks, and special bibliographies.

TECHNOLOGY UTILIZATION PUBLICATIONS: Information on technology used by NASA that may be of particular interest in commercial and other non-aerospace applications. Publications include Tech Briefs, Technology Utilization Reports and Notes, and Technology Surveys.

Details on the availability of these publications may be obtained from:

SCIENTIFIC AND TECHNICAL INFORMATION DIVISION

NATIONAL AERONAUTICS AND SPACE ADMINISTRATION

Washington, D.C. 20546